

**PREPARATION OF A LAB SCALE EXTRUDER MACHINE AND INVESTIGATION OF  
THE PERIODIC SURFACE DISTORTIONS IN EXTRUSION OF POLYOLEFINS AND  
USAGE OF NOVEL PROCESSING AIDS TO OVERCOME THESE INSTABILITIES**

**M.Sc. Thesis by  
Ahmet MERİÇ**

**Department : Polymer Science and Technology**

**Programme: Polymer Science and Technology**

**MAY 2005**

**İSTANBUL TEKNİK ÜNİVERSİTESİ ★ FEN BİLİMLERİ ENSTİTÜSÜ**

**LABORATUVAR BOYUTUNDA BİR EKSTRUDER MAKİNESİNİN HAZIRLANMASI  
VE POLİOLEFİNLERİN EKSTRUZYONUNDA GÖRÜLEN PERİYODİK BİÇİM  
BOZUKLUKLARININ YENİ PROSES İYİLEŞTİRİCİLER İLE GİDERİLMESİ**

**YÜKSEK LİSANS TEZİ  
Ahmet MERİÇ  
515011002**

**Anabilim Dalı : Polimer Bilimi ve Teknolojisi**

**Programı : Polimer Bilimi ve Teknolojisi**

**Tez Danışmanı: Prof. Dr. Nurseli UYANIK**

**MAYIS 2005**

**PREPARATION OF A LAB SCALE EXTRUDER MACHINE AND INVESTIGATION OF  
THE PERIODIC SURFACE DISTORTIONS IN EXTRUSION OF POLYOLEFINS AND  
USAGE OF NOVEL PROCESSING AIDS TO OVERCOME THESE INSTABILITIES**

**M.Sc. Thesis by  
Ahmet MERİÇ  
515011002**

**Department : Polymer Science and technology**

**Programme: Polymer Science and technology**

**Supervisor : Prof. Dr. Nurseli UYANIK**

**MAY 2005**

## **ACKNOWLEDGMENT**

Above all, I gladly thank my dear advisors Prof. Dr. Nurseli UYANIK and Dr. Meral KAYA who helped me willingly with their knowledge and support whenever I needed during my thesis study.

I also thank Yılmaz Redüktör Inc., Medel Inc., Safi Rezistans Inc., Omega Inc., Aksoy Plastics Inc. who helped me with the equipment they supplied during the preparation of the extruder. Thanks to Ayhan EZDEŞİR from PETKİM for the support regarding to rheological tests. Technical Manager of Enformak PT Inc. Güneri ARCAN, my father Şerif MERİÇ who helped me with their knowledge and support and all the staff of Enformak Inc. during the production of the extruder

Besides, I specially thank my dear wife Figen MERİÇ, who continuously encouraged and inspired me, for her endless patience and spiritual support.

Finally, lots of thanks to my dear mother, -again- father and brother for their endless support during my whole life.

May 2005

Ahmet MERİÇ

<b>ACKNOWLEDGMENT</b>	<b>ii</b>
<b>INDEX</b>	<b>iii</b>
<b>TABLE LIST</b>	<b>vi</b>
<b>FIGURE LIST</b>	<b>vii</b>
<b>SYMBOL LIST</b>	<b>viii</b>
<b>ÖZET</b>	<b>x</b>
<b>SUMMARY</b>	<b>xv</b>
 <b>1.INTRODUCTION</b>	 <b>1</b>
 <b>2.THEORY</b>	 <b>4</b>
<b>2.1. Extruder</b>	<b>4</b>
2.1.1. Ram Extruder	4
2.1.2 Disk Extruders	5
2.1.2.1 Viscous Drag Disk Extruders	5
2.1.2.2 The Elastic Melt Extruder	6
2.1.3. Screw Extruders	6
2.1.3.1 Single Screw Extruders	6
2.1.3.2. Basic Operation	7
2.1.3.3. Vented Extruders	8
2.1.3.4. Rubber Extruders	9
2.1.3.5 The Multi screw Extruder	9
2.1.3.6. The Twin Screw Extruder	9
2.1.3.7. The Multi Screw Extruder with More Than Two Screws	11
<b>2.2 Design of a Single Screw Extruder</b>	<b>11</b>
2.2.1 Rheology of a Polymer Melt	11
2.2.1.1 Viscous Behavior of Polymer Melt	13
2.2.1.2 Plasticating Single-Screw Extruders	18
2.2.1.3 Solids Transport	18
2.2.1.4 Delay and Melting Zones	21
2.2.1.5 Metering zones	23
 <b>2.3 Polyolefins</b>	 <b>26</b>

2.3.1 Polyethylenes and ethylene copolymers	26
2.3.1.1 LLDPE (Linear Low Density Polyethylene)	28
2.3.1.2 Very Low Density Polyethylene	29
2.3.1.3 HMW High Density Polyethylene	29
2.3.1.4 Ethylene-methyl-acrylate	29
2.3.1.5 Ethylene-ethyl-acrylate	30
2.3.1.6 Ethylene-vinyl-acetate	30
2.3.1.7 UMHW Polyethylene	30
2.3.2 Polypropylene	30
<b>2.4 Extrudate flow instabilities</b>	<b>32</b>
<b>3. EXPERIMENTAL</b>	<b>37</b>
<b>3.1. Preparation of the laboratory extruder</b>	<b>37</b>
3.1.1. Design of screw and barrel	38
3.1.2. Material used in preparation of screw and barrel	38
3.1.3. The main components of the extruder	38
3.1.3.1 Motor	38
3.1.3.2 Reduction gear box	39
3.1.3.3. Heaters and coolers	39
3.1.3.4. Pressure Gauge	39
3.1.3.5. Control board	40
3.1.4. Construction of the Extruder	40
<b>3.2. Experimental Study of Surface Irregularities</b>	<b>40</b>
3.2.1. Materials Used for Surface irregularities study	40
3.2.1.1 LDPE	40
3.2.1.2 Commercial Polymer Processing Aid (PPA) Additives	40
3.2.1.3 Silicone Based Additive	41
3.2.2. Equipments	41
3.2.2.1 Extruder	41
3.2.2.2 Die	41
3.2.2.3 Melt Flow Index Equipment	41
3.2.2.4 Camera	41

3.2.2.5 Parallel Plate Rheometer	42
3.2.3. Experimental Method	42
3.2.3.1 Calculation of the shear stress	42
3.2.3.2 Determination of Critical Shear Stress Value	42
3.2.3.3 Effects of Commercial Additives	44
3.2.3.4 Effects of of silicone based Additives	45
3.2.3.5 Comparison of the Samples Regarding to Rheological Properties	46
<b>4. RESULTS AND DISCUSSION</b>	<b>47</b>
4.1 Preperation of the laboratory extruder	47
4.2 Determination of Critical Shear Stress Value	47
4.3 Effects of Commercial Additives	47
4.4 Effects of Silicone Based Additives	48
4.5 MFR Measurements	48
4.6 Rheological Properties	49
4.7 Conclusion	51
<b>REFERENCES</b>	<b>52</b>
<b>APPENDIX</b>	<b>55</b>
<b>CURRICULUM VITAE</b>	<b>69</b>

## TABLE LIST

	<b><u>Page</u></b>
<b>Table 2.1.</b> Types of twin screw extruders .....	10
<b>Table 2.2.</b> Summary of methods for measuring viscosity .....	12
<b>Table 2.3.</b> Flow models and equations.....	16
<b>Table 2.4.</b> Classification of the Polyethylenes. ....	27
<b>Table 3.1.</b> Temperature profile and extrusion data's of LDPE with 190 C° Die Temp.....	43
<b>Table 3.2.</b> Temperature profile and extrusion data of LDPE with 175 C° Die Temp.....	44
<b>Table 3.3.</b> Temperature profile and extrusion data of LDPE with different additive ratios.....	45
<b>Table 3.4.</b> Temperature profile and extrusion data of LDPE- H-Si 6440 with different ratio and shear rates.....	46
<b>Table 4.1.</b> Calculated and experimental mass flow rate.....	55
<b>Table 4.2.</b> Surface conditions of LDPE at different shear stress.....	56
<b>Table 4.3.</b> Surface conditions of LDPE – Dyneon additives mixture at different shear stress. ....	57
<b>Table 4.4.</b> Surface conditions of LDPE – H-Si 6440 additives mixture at different shear stress. ....	58
<b>Table 4.5.</b> MFI and MFR results of the LDPE, FX 5920 and H-Si 6440 mixtures. ....	59



## FIGURE LIST

	<u>Page</u>
<b>Figure 2.1</b> : Single ram and twin ram extruder.....	5
<b>Figure 2.2</b> : The drum disk extruder by Schmid & Kocher and Asco & Cosden.....	5
<b>Figure 2.3</b> : Schematic drawing of conventional plasticating single screw extruder.....	6
<b>Figure 2.4</b> : Counter rotating conical twin screw.....	10
<b>Figure 2.5</b> : Co-rotating parallel twin screw .....	10
<b>Figure 2.6</b> : Steady simple shear flow with shear rate = $V/b$ .....	13
<b>Figure 2.7</b> : Viscous response of Non Newtonian fluids.....	14
<b>Figure 2.8</b> : Rectangular channel filled with granular solids with a plate moving at angle $\Phi$ relative to the down channel direction.....	18
<b>Figure 2.9</b> : Motion of the plate relative to motion of the solid bed. The plate moves at an angle $\Phi'$ relative to solid bed.....	19
<b>Figure 2.10</b> : LLDPE extrudate displaying sharkskin $V/D= 985$ .....	33
<b>Figure 2.11</b> : LLDPE extrudate displaying wavy fracture 8 $V/D= 6155$ .....	33
<b>Figure 3.1</b> : Constructional drawing of the extruder.....	37
<b>Figure 3.2</b> : Design of the screw .....	38
<b>Figure 3.3</b> : Components of the extruder .....	39
<b>Figure 3.4</b> : Shape of the slit die used.....	42
<b>Figure 3.5</b> : Shear stress vs. Screw speed graph for LDPE at 175 and 190 °C. 44	
<b>Figure 4.1</b> : Surface appearance of the extruded LDPE slits in different die pressures.1; 70 Bar, 2; 90 Bar, 3:110 Bar, 4; 161 Bar.....	60
<b>Figure 4.2</b> : Surface appearance of the extruded samples in same shear stress point 1. LDPE at 110 Bar, 2.1500 PPM FX 5920 at 110 Bar, 3.750 PPM H-Si 6440 at 110 bar.....	61
<b>Figure 4.3</b> : Viscosity vs. shear rate plot.....	62
<b>Figure 4.4</b> : Viscosity vs. shear stress plot.....	63
<b>Figure 4.5</b> : Shear stress vs. Shear rate plot.....	64
<b>Figure 4.6</b> : Storage modulus $G'$ vs. Angular frequency $\omega$ plot.....	65
<b>Figure 4.7</b> : Loss modulus $G''$ vs. Angular frequency $\omega$ plot.....	66
<b>Figure 4.8</b> : Storage modulus $G'$ vs. loss modulus $G''$ plot.....	67
<b>Figure 4.9</b> : Complex viscosity $ \eta^* $ vs. Angular frequency plot.....	68

## SYMBOL LIST

<b>F</b>	: Force
<b>A</b>	: Area of the plates
<b><math>\mu</math></b>	: Viscosity of the fluid
<b>V</b>	: Velocity
<b>H</b>	: Separation distance
<b><math>\dot{\gamma}</math></b>	: Shear rate
<b><math>\tau</math></b>	: Shear stress
<b><math>\eta</math></b>	: Shear viscosity
<b>m</b>	: Consistency
<b>n</b>	: Power-law index
<b><math>\lambda</math></b>	: $\sim 1/\dot{\gamma}$ for the onset of shear thinning
<b><math>m'</math></b>	: Power-law parameter in Hershel-Bulkley model
<b><math>V_r</math></b>	: Velocity of plate relative to solid bed
<b><math>\Phi</math></b>	: Helix angle
<b>K</b>	: Anisotropy in the stress distribution
<b><math>f_w</math></b>	: Friction coefficient
<b>G</b>	: Mass flow rate
<b><math>V_{pl}</math></b>	: Plug velocity
<b><math>D_b</math></b>	: Barrel diameter
<b><math>D_s</math></b>	: Screw diameter
<b><math>V_b</math></b>	: Velocity of barrel surface
<b><math>\Phi_b</math></b>	: Helix angle of barrel surface
<b>N</b>	: Angular velocity of screw, rad/s
<b>e</b>	: Flight width
<b>M</b>	: Degree of mixing
<b>W</b>	: Width of channel
<b><math>P_w</math></b>	: Power input through barrel
<b><math>W_b</math></b>	: Channel width at barrel surface
<b><math>Z_b</math></b>	: Down channel distance
<b><math>\overline{C}_{p.p}</math></b>	: Heat capacity
<b><math>k_p</math></b>	: Thermal conductivity
<b><math>T_p</math></b>	: Temperature in plug
<b><math>\alpha_p</math></b>	: Thermal diffusivity
<b><math>\overline{C}_p</math></b>	: Constant pressure heat capacity per unit mass
<b><math>\Delta \overline{H}_f</math></b>	: Heat of fusion
<b>X</b>	: Width of the solid bed
<b><math>\Psi</math></b>	: Dimensionless variable in melting model
<b>Q</b>	: Volumetric flow rate
<b><math>Q_p</math></b>	: Pressure flow
<b><math>Q_d</math></b>	: Drag flow
<b><math>Q_s</math></b>	: Volumetric flow in the extruder

**$\Delta P$**  : Internal overpressure  
**L** : Length

# **PREPARATION OF A LAB SCALE EXTRUDER MACHINE AND INVESTIGATION OF THE PERIODIC SURFACE DISTORTIONS IN EXTRUSION OF POLYOLEFINS AND USAGE OF NOVEL PROCESSING AIDS TO OVERCOME THESE INSTABILITIES**

## **SUMMARY**

80% of the plastics consumption of the world is thermoplastics. The Polyolefins are the widely used one of this percentage. These polymers consist of Polyethylenes, Polypropylenes, Polybutenes and Polyisoprenes, formed from the corresponding olefins by an addition polymerization process

Polyolefins are especially used in extrusion process in the industry. The extruder is indisputably the most important piece of machinery in the polymer processing industry. The largest volume of thermoplastics is probably processed by means of extrusion. To extrude means to push or to force out. Material is extruded when it is pushed through an opening. When toothpaste is squeezed out of a tube, it is extruded.

The plasticating extruder performs three actions in process. It melts or plasticates the material, it generates the pressure on the material to force it through to die orifice, and it shears and mixes the material.

Polymer extrudate flow exhibits instabilities under sufficiently high stress. In the case of linear polymers such as high-density polyethylenes, the first appearance of instability is periodic small-amplitude distortion of the extrudate surface. This instability is referred to as sharkskin fracture, and has been discussed in relation to various aspects

Regular surface irregularities generated at the melt/metal interface especially at higher extrusion rates which is above critical shear stress point. Hence these surface irregularities which are undesired are a limiting factor for extrusion manufacturing speed of the polyolefinic thermoplastics. If it's provided to move this critical shear stress value to higher points, this will mean that: polyolefinic products will be produced with higher productivity.

With this project, a lab scale single screw extruder machine will be prepared to study the experiments of polyolefin extrusion. Surface irregularities of the LDPE (Low Density Polyethylene) will be studied and it was tried to be eliminated by using commercial processing aids. In addition to this, a novel processing aid containing silicone was tested for the elimination of the irregularities.

The extruders in the polymer industry come in many different designs. The main distinction between the various extruders is their mode of operation: continuous or discontinuous. The latter type extruder delivers polymer in an intermittent fashion and, therefore, is ideally suited for batch type processors, such as injection molding and blow molding.

The main types of extruders are;

— Ram extruders

- Disk extruders
- Screw Extruders

The transport properties of polymeric materials, which can distinguish them most from other materials, are their flow properties or rheological behavior. There are many differences between the flow properties of a polymeric fluid and typical low-molecular-weight fluids such as water, benzene, sulfuric acid, and other fluids that we classify as Newtonian. Newtonian fluids can be characterized by a single flow property called viscosity ( $\mu$ ) and by density ( $\rho$ ). Polymeric fluids, on the other hand, exhibit a viscosity function that depends on shear rate or shear stress, time-dependent rheological properties, viscoelastic behavior such as elastic recoil (memory), additional normal stresses in shear flow, and an extensional viscosity not simply related to the shear viscosity to name a few differences.

A single screw extruder has been modeled mathematically. 3 stages of the screw have been modeled. Feeding section, melting and delaying section and also the metering section have been modeled for the Newtonian case.

Polyethylene and the other polyolefins are explained in general terms.

Literature has been investigated regarding to sharkskin, melt fracture phenomena. A brief explanation about the studies has been written.

Experimental studies were done in two main subjects; preparation of a lab scale extruder machine and investigation of the periodic surface distortions in extrusion of polyolefins and usage of novel processing aids to overcome these instabilities.

In order to make the surface distortion experiments; we prepared an extruder as a part of this study. We intended to design the extruder as a universal laboratory extruder which can be run with various types, small quantity experiment samples. The design of the extruder screw and the barrel and the constructional design of the extruder were made as a part of this study.

The extruder, which is designed and produced as a part of this study (**Figure1**), was used for the investigation of the surface irregularities. Two different dies attached to the extruder were used. A die was used to have compounded strands and another rectangular slit die was used to carry out surface irregularities studies. The length of the land region of the slit die, land region length  $L$ , is 28 mm, width of the die,  $W$ , is 25 mm and the thickness,  $H$ , is 1 mm.

Low density polyethylene used is a commercial product of Petkim Petilen G 03-5. Dyneon FX 5920 PPA and Dyneon FX 9613 PPA were used to see the effects of commercial processing aids. The  $\alpha$ ,  $\omega$  dihydroxy polycaprolactone-poly (dimethylsiloxane) (PCL-PDMS-PCL) triblock copolymer used was a commercial product Goldschmidt Chemical Corp. and was tested as a novel processing aid.

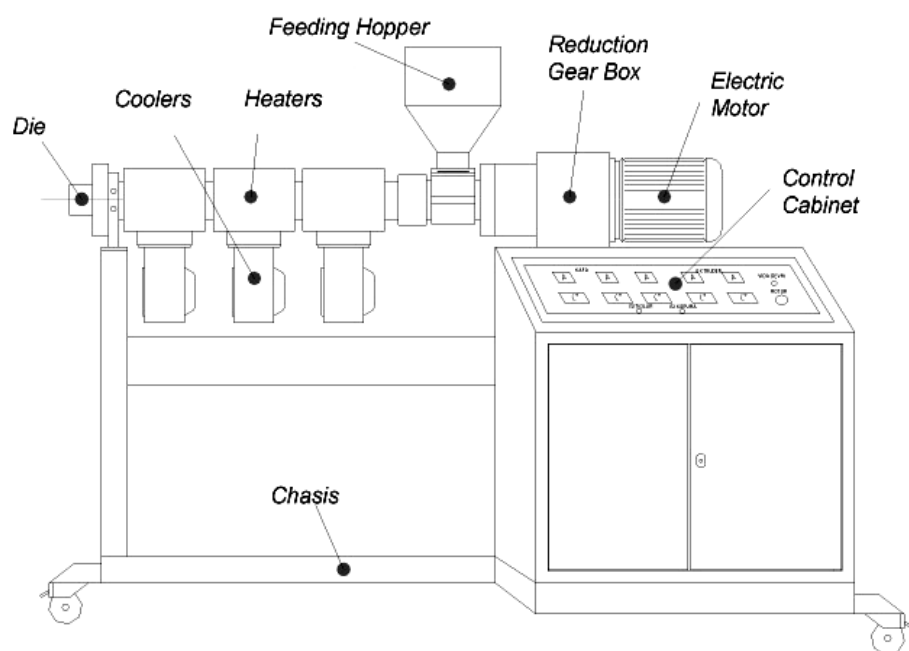


**Figure 1:** Components of the prepared extruder

For the observation of results, execution of a MFR measurement was described in DIN ISO 1133 as procedure. High resolution 5.1 mega pixel Sony DCR-W digital camera which has close-up mode was used to picture the surface conditions of the samples.

In order to determine the critical shear stress approximate value of 0.1, MPa that was stated in the literature was tested. For this purpose LDPE was extruded by the slit die under different extrusion rates (**Figure2**).

Up to 70 bar die pressure, almost no surface defect has been seen. After the 70 bar die pressure, the screw speed has been increased step by step (Table1).

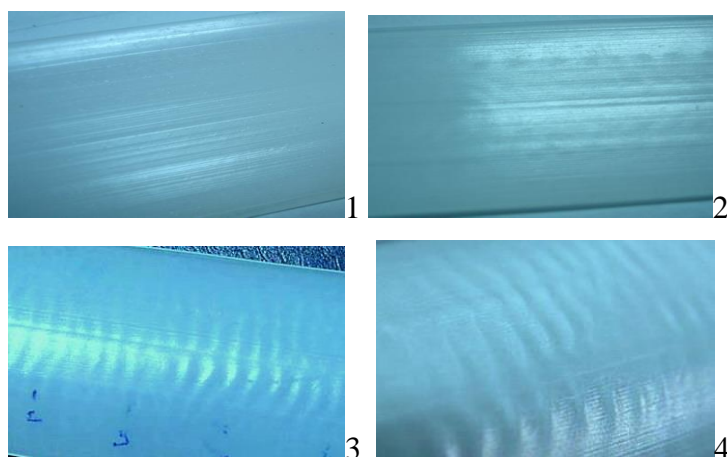


**Figure 2:** Surface appearance of the extruded LDPE slits in different die pressures.1; 70 Bar, 2; 90 Bar, 3;110 Bar, 4; 161 Bar

Some small amplitude sharkskin melt fracture defect has been seen at the shear stress value of 1,66 MPa. As it is mentioned in Section 2.4; “during extrusion, at a critical wall shear stress greater than about 0.1 MPa, fine-scale surface irregularities appears, commonly known as “sharkskin”. We almost got the same result.

In order to see the effects of the commercial processing aids, we used Dyneon processing aids in different ratios. We also tried the H-Si 6440 as a novel processing aid because of its similar properties (**Figure3**).

**Table 1:** Extrusion of LDPE with different extrusion rates.

Die (C°)	3. Zone (C°)	2. Zone (C°)	1. Zone (C°)	
190	190	180	140	
Material	Screw Speed (r.p.m)	$\Delta P$ Die Pressure (Bar)	Calc. Shear Stress (MPa)	Surface Condition Comment
LDPE	6	70	0,120	Almost no surface defect
LDPE	10	90	0,154	Some small sharkskin effect started
LDPE	15	102	0,175	Sharkskin effect has been seen
LDPE	20	110	0,188	Sharkskin effect has been seen
LDPE	25	119	0,204	Sharkskin effect markedly increased
LDPE	30	125	0,214	Sharkskin effect markedly increased
LDPE	44	161	0,276	Extrudate unstable, Gross irregularities near



**Figure 3:** Surface appearance of the extruded samples in same shear stress point 1. LDPE at 110 Bar, 2.1500 PPM FX 5920 at 110 Bar, 3.750 PPM H-Si 6440 at 110 bar.

When we compare the melt flow rates, it has been seen that both samples have higher MFR values than the pure LDPE has, and there is no significant difference among results. The rheometer test results showed that; all the samples showed the pseudoplastic behavior and both of the samples has higher zero shear viscosity, and the H-Si 6440 has the highest one. The 0.5 rad/s frequency value showed a boundary

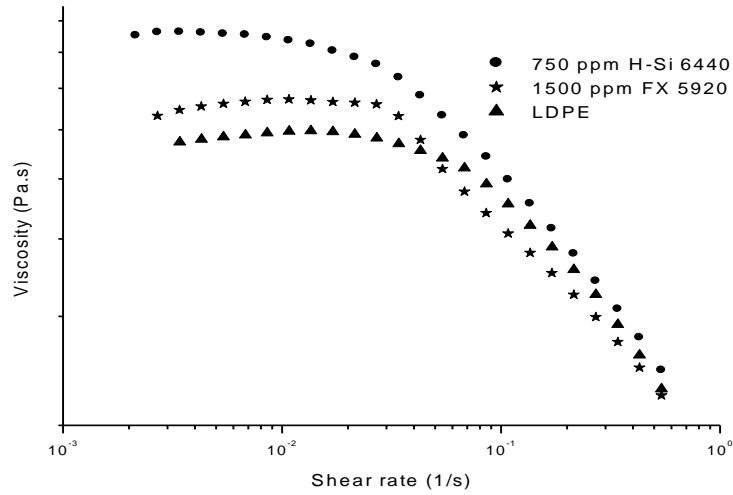


**Figure 4:** Viscosity vs. shear rate plot

on the all rheometer test plots. This 0,5 rad/s value can be say as the boundary of Newtonian and Pseudoplastic region (**Figure4**).

It has been seen that; Dyneon processing aids helped to have better surface conditions above the critical shear stress value. The H-Si 6440 has also showed similar advantages regarding the sharkskin melt fracture. It has also been seen that; it also has some advantages such as lower usage level.



# **LABORATUVAR BOYUTUNDA BİR EKSTRUDER MAKİNESİNİN HAZIRLANMASI VE POLİOLEFİNLERİN EKSTRUZYONUNDA PERYODİK BİÇİM BOZUKLUKLARININ YENİ PROSES İYİLESTİRİCİLER İLE GİDERİLMESİ**

## **ÖZET**

Dünyada kullanılan plastiklerin % 80'i termoplastik malzemelerdir. Poliolefinler ise bu sınıfın en yaygın kullanılan grubunu teşkil eder. Bu polimerler Polietilen, polipropilen, Polibütan ve polisopren gibi polimerlerdir. İlgili olefinlerin katılma tepkimesi ile polimerleşirler.

Poliolefinler özellikle endüstride ekstrüzyon ile işlemede kullanılırlar. Extruderler şüphesiz plastik işleme sektöründeki en önemli makinelerdir . Plastik endüstrisindeki ürünlerin büyük kısmı ekstruderler vasıtasıyla şekillendirilir. 'Extrude' kelimesi zorlayıp, basınçla dışarı çıkarmak manasına gelmektedir. Malzeme bir açıklıktan zorla bastırılarak çıkarıldığında 'extrude' edilmiş olur.Buna bir örnek diş macununu sıkarak tüpten çıkarmaktır.

Plastik ekstruderleri kabaca üç işlem gerçekleştirirler. Malzemeyi eritir, kalıptan dışarı çıkarmak için gereken basıncı oluşturur ve eriyik plastiği karıştırıp gereken gerilimi oluştururlar.

Polimer ekstruder ürünleri yeterince yüksek basınç altında aktıkları zaman akış kararsızlıkları gösterirler.Yüksek yoğunluklu polietilen gibi lineer polimerlerde bu kararsızlıkların ilk görünüm şekli ürünün yüzeyindeki küçük periyodik genişlemelerdir. Bu kararsızlık köpekbalığı derisi kırılması olarak adlandırılır ve bir çok yönüyle araştırmalara konu olmuştur.

Periyodik yüzey bozuklukları eriyik metal ara yüzeyinde oluşur ve özellikle kritik kesme gerilimi üzerindeki ekstrüzyon hızlarında ortaya çıkmaktadır. Bu nedenle bu tür yüzey bozuklukları poliolefinlerin ekstrüzyonla şekillendirilmesi işleminde, üretim hızını engelleyen bir faktördür. Eğer kritik kesme gerilimi değeri daha yukarılara çekilebilirse, bu poliolefinlerin ekstruderle şekillendirilmesinin daha yüksek hızlarda yapılabileceği manasına gelecektir.

Bu çalışmanın bir parçası olarak öncelikle poliolefinlerin ekstrüzyonu ile ilgili çalışmak adına laboratuvar düzeyinde bir ekstruder hazırlanacaktır. Alçak Yoğunluklu Polietilen (AYPE) nin ekstrüzyonla üretimdeki yüzey bozuklukları incelenecek ve bu bozuklukların ticari katkılar aracılığıyla düzeltilmesine çalışılacaktır. Bununla birlikte silikon içeren yeni bir katkı maddesinin yüzey bozukluklarına karşı etkisi incelenecektir.

Ekstruderler polimer endüstrisinde çok farklı dizaynlarla ortaya çıkmaktadır. Bu çok fazla çeşidin içinde ana ayırım noktası, çalışma biçimleridir; sürekli ve süreksiz çalışanlar. Sonraları üretilen ekstruderler aralıklı periyotlarla ürün verebildiği için daha çok enjeksiyon veya şişirme yöntemiyle şekillendirme operasyonlarında kullanılırlar. Temel ekstruder çeşitleri;

- Piston tipi ekstruderler
- Disk ekstruderler

## — Vidalı ekstruderler

Polimerleri diğer bir çok malzemelerden ayıran nakil özellikleri, reolojik akış özellikleridir. Polimerik akışkanları diğer alçak moleküler ağırlıklı, su, benzen, sülfirik asid gibi Newton akışkanı olarak değerlendirilen akışkanlardan ayıran birçok akış özelliği vardır. Newton akışkanları viskozite olarak adlandırılan bir tek akış özelliği ve yoğunlukla ifade edilebilirler. Diğer taraftan polimerik akışkanlarda zamanla değişen, kesme gerilimine ve kesme oranına bağlı reolojik özellikler, viskoelastik tavır, elastik geri tepme (hafıza), kesme akışlarında fazladan normal gerilim ve uzama viskozitesi gibi diğer faktörler kolaylıkla kesme viskozitesi ile bağdaştırılıp, önemsiz birkaç farklılık gibi görülemez. Polimerlerin reolojik özellikleri teorik kısımda daha detaylı incelendi.

Bir tek vidalı ekstruder teorik kısımda matematiksel olarak modellendi. Vidanın üç bölgesi besleme, eritme ve basınç bölgeleri Newton akışkanları için modellendi.

Polietilen ve diğer bazı poliolefinler kısaca anlatıldı.

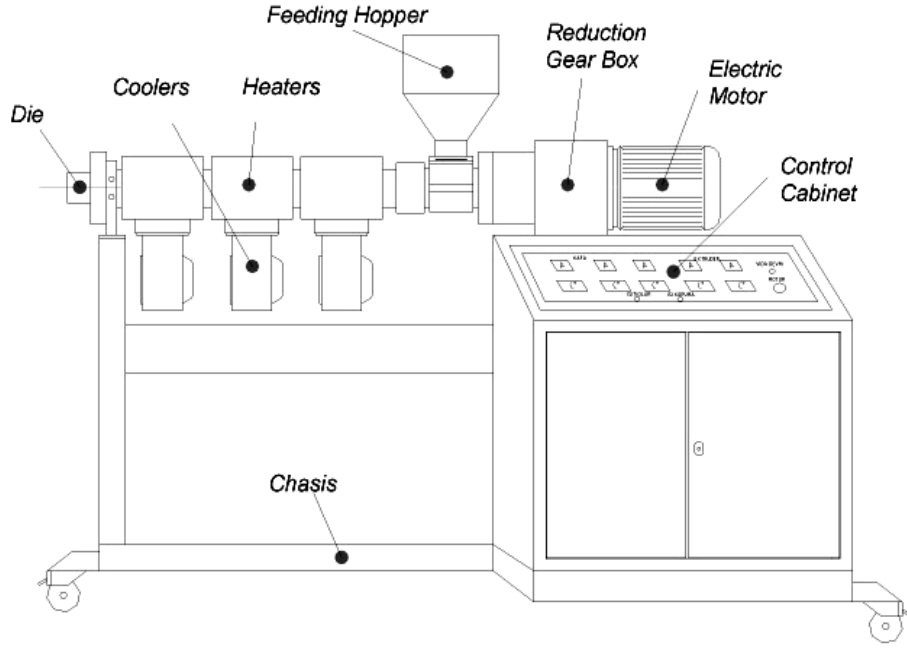
Literatürdeki köpekbalığı derisi eriyik kırılması çalışmaları incelendi ve bu konuyla ilgili çalışmalar kısaca anlatıldı.

Deneysel çalışmalar iki ana başlık altında yapıldı; Laboratuvar boyutlarında bir tek vidalı ekstruderin hazırlanması ve poliolefinlerin ekstrüzyonundaki yüzey bozukluklarının incelenerek yeni işleme yardımcıları ile giderilmesini sağlamak.

Yüzey bozuklukları çalışmalarını yapabilmek için tek vidalı bir ekstruder çalışmanın bir parçası olarak hazırlandı. Laboratuvarında çeşitli çalışmalarda kullanılabilmesi adına çeşitli polimerlerle ve az miktarda numune çalışabilecek bir ekstruder dizayn edilmeye çalışıldı. Extruderin konstrüksiyon çalışması ve kovan ve vidanın dizaynı çalışma kapsamında geliştirildi.

Yüzey bozukluğu çalışmalarında çalışma kapsamında hazırlanmış olan ekstruder kullanıldı (**Şekil 1**), Ekstruderle beraber çalışmalarda iki farklı kalıp kullanıldı. Gereken karışımı granül olarak elde edebilmek için bir granül kalıbı ve yüzey bozukluğu çalışmalarını yapmak adına ütüleme boyu (L) 28 mm , genişliği (W) 25 mm ve kalınlığı (H) 1mm olan bir şerit kalıbı.

Petkim'in ticari bir polimeri olan Petilen G-03-5 Alçak Yoğunluklu Polietilen (AYPE), Dyneon FX 5920 PPA ve Dyneon FX 9613 PPA ticari katkıları iyileştiricilerin etkisini görmek üzere,  $\alpha$ ,  $\omega$  dihidroksi polikaprolakton-poli (dimetil siloksan) ( PCL-PDMS-PCL) Goldschmidt Chemical firmasının üç bloklu ticari kopolimeri silikonun etkisini görebilmek üzere yeni işleme yardımcısı olarak yüzey bozukluğu çalışmalarında test edildi.

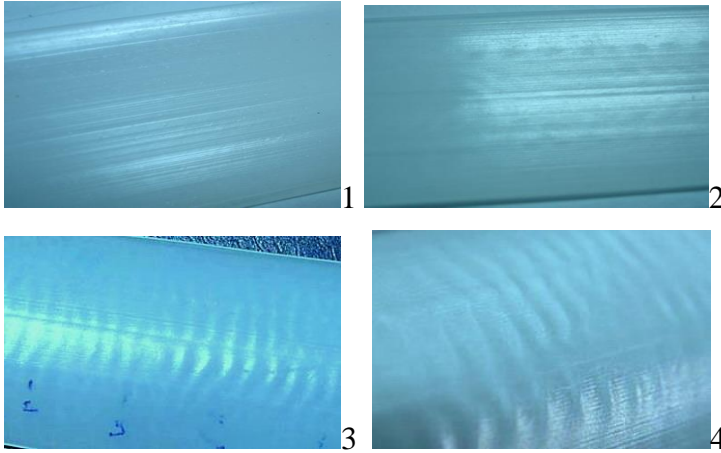


**Şekil 1:** Ekstruderi oluşturan bileşenler

Neticelerin değerlendirilmesi için MFR ölçümleri DIN ISO 1133 prosedürüne göre yapıldı. Yüksek çözünürlüklü yakın çekim yapma özelliğine sahip 5.1 mega piksel Sony DCR-W fotoğraf makinesi yüzey bozuklukları ile ilgili çalışmaları resimlemek için kullanıldı.

Literatürde geçen kiritik kesme gerilimi değeri (0,1 MPa) test edildi. Bu amaçla LDPE şerit kalıbı ile farklı ekstruder hızları kullanılarak denendi. (Şekil 2)

70 bar kalıp basıncına kadar herhangi bir yüzey bozunması gözlemlenemedi. 70 bar basıncın üzerinde ekstruder hızı adım adım artırıldı.(Tablo1)



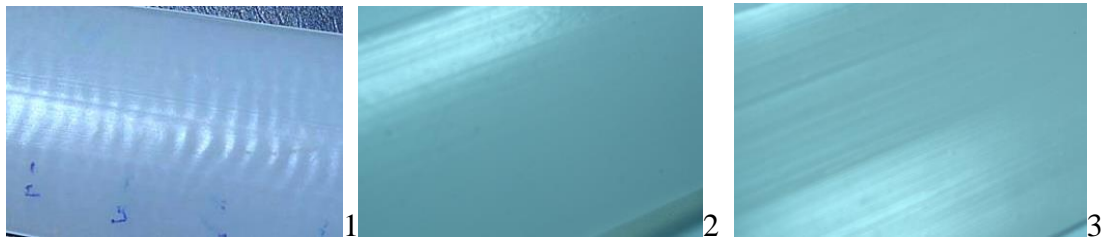
**Şekil 2:** Ekstruderde değişik kalıp basınçları altında çekilen LDPE şeritle.1. 70 Bar, 2. 90 Bar, 3.110 Bar, 4. 161 Bar

Bazı ufak boyutlu köpekbalığı derisi eriyik kırılması bozunmaları 1,66 MPa kesme gerilimi değerinde ortaya çıkmaya başladı. Bölüm 2.4’te bahsedildiği gibi “0,1 MPa değeri üzerindeki kritik kesme gerilimlerinde ince aralıklarla başlayan bozunmalar köpekbalığı derisi bozunması olarak bilinir” ifadesi bizim çalışmamızda da doğrulandı.

Dyneon Ticari katkıları ve H-Si 6440 silikon içerikli katkısının yüzey bozukluklarına etkisini görmek üzere bu iki malzeme çeşitli ekstrüzyon hızlarında test edildi (**Şekil 3**).

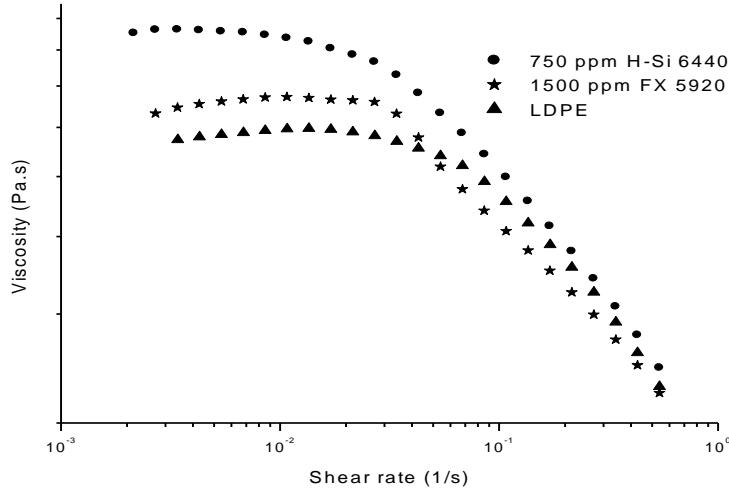
**Tablo 1:** LDPE ‘nin değişik ekstrüzyon hızlarında denenmesi

Kalıp (C°)	3. Bölge (C°)	2. Bölge (C°)	1. Bölge (C°)	
190	190	180	140	
Malzeme	Vida Hızı (r.p.m)	$\Delta P$ Kalıp Basıncı (Bar)	Hes. Kesme Gerilimi (MPa)	Yüzey durumu
LDPE	6	70	0,120	Hemen hemen hiç bozunma yok
LDPE	10	90	0,154	Bazı ufak Köpekbalığı derisi etkileri görülmeye başladı
LDPE	15	102	0,175	Köpekbalığı derisi etkisi görüldü.
LDPE	20	110	0,188	Köpekbalığı derisi etkisi görüldü.
LDPE	25	119	0,204	Köpekbalığı derisi etkisi artarak görüldü.
LDPE	30	125	0,214	Köpekbalığı derisi etkisi artarak görüldü.
LDPE	44	161	0,276	Çekilen şerit karasız hale gelmeye yaklaştı.



**Şekil 3:** Aynı kesme gerilimi altında numunelerin yüzey görünüşleri **1.**LDPE,110 Bar, **2.**1500 PPM FX 5920,110 Bar, **3.**750 PPM H-Si 6440 at 110 bar.

Eriyik akış indeksi değerleri incelendiğinde, iki katkı örneğinin değerleri de saf LDPE nin değerinden yüksek olduğu fakat değerler arasında önemli bir fark olmadığı



**Şekil 4:** Viskosite vs. kesme oranı grafiği

görülmüştür. Reometre ile yapılan test neticelerinde bütün örneklerin ‘psuedoplastic’ tavrı izlediği görülmüştür. Katkıların ikisinin de sıfır kesme vizkosite değerlerinin saf LDPE den fazla olduğu, H-Si 6440 katkılı LDPE nin ise en büyük sıfır kesme vizkositesine sahip olduğu görülmüştür. 0.5 rad/s frekans değeri reoloji testi sonuç grafiklerinde bir sınır değeri gösterdi. Bu değerin örneklerin Newton akışı ve Newton dışı (pseudoplastic) bölgeler arasındaki geçiş değeri olduğu söylenebilir (**Şekil 4**).

Dyneon ticari katkılarının kritik kesme gerilimi üzerinde daha iyi yüzeyler elde etmeye yardımcı olduğu tespit edildi. H-Si 6440 benzer özellikler göstererek köpekbalığı derisi yüzey bozukluklarını azalttı. Bununla beraber daha az oranda kullanım gibi bir takım avantajlar sağladığı da görüldü.

## **1. INTRODUCTION**

The extruder is indisputably the most important piece of machinery in the polymer processing industry. The largest volume of thermoplastics is probably processed by means of extrusion. To extrude means to push or to force out. Material is extruded when it is pushed through an opening. When toothpaste is squeezed out of a tube, it is extruded. The part of the machine containing the opening through which the material is forced is referred to as an extruder die. As material passes through the die, the material acquires the shape of the die opening. This shape generally changes to some extent as the material exits from the die.

There are two basic types of extruders: continuous and discontinuous, or batch type extruders.

Continuous extruders are capable of developing a steady, continuous flow of material, whereas batch extruders operate in a cyclic fashion. Continuous extruders utilize a rotating member for transport of the material. Batch extruders generally have a reciprocating member to cause the transport of the material.

Many different materials are formed through an extrusion process; metals, clays, ceramics, foodstuffs, etc. The food industry, in particular, makes frequent use of extruders to make noodles, sausages, snacks, cereal, and numerous other items.

As it is used for other industries, extruders are the heart of the polymer processing industry. They are used at some stage nearly in all polymer processing such as plastic sheet, film, pipe, hose, profiles etc. Although the main function of the single screw extruder is to melt and pump polymer, there are a number of other applications. Extruders can be used to remove volatiles such as water or trace amounts of monomers. They can be used to generate foamed polymers as the temperature and pressure history can be controlled. They also serve as continuous mixing and compounding devices. Hence, extruders have a wider range of applications.

The plasticating extruder performs three actions in process. It melts or plasticates the material, it generates the pressure on the material to force it through to die orifice, and it shears and mixes the material.

There are basically three classifications of extruders; screw extruders, disk extruders, and ram extruders. The most common ones are the screw extruders. The screw extruders, which are commonly used in practice, can be categorized basically in two groups; single screw extruders and twin-screw extruders. The most common screw extruders are the single screw extruders. For this reason it has been emphasized and a lab scale single screw extruder has been prepared to use in the laboratory.

The use of a single screw extruder to produce extrudate products has some limitations. It is not possible to produce the extrudate product with limitless speed. Manufacturers specifically wish to increase the flow rate, reduce energy cost, and minimize the occurrence of extrudate irregularities. Some surface distortions limit the extrusion process when the extrusion speed exceeds these limiting velocities.

80% of the plastics consumption of the world is thermoplastics. And most of them are the olefinic polymers which are called 'polyolefines'. Polyolefines are the widely used ones of this percentage. Polyolefines are especially used in extrusion process in industry. These polymers consist of Polyethylenes, Polypropylenes, Polybutenes and Polyisoprenes, formed from the corresponding olefins by an addition polymerization process [1].

Extrudate irregularities have been studied for more than 50 years on a wide range of polymers and especially on polyolefines. The quality of a polymer extrudate depends on the flow defects during polymer melt extrusion, a subject which has received considerable attention in the literature, in particular as to what 'melt fracture' and 'sharkskin' instabilities of polyethylenes are. The influences of structure, capillary geometry, and operating variables have been investigated.

Polymer extrudate flow exhibits instabilities under sufficiently high stress. In the case of linear polymers such as high-density polyethylenes, the first appearance of the instability is periodic small-amplitude distortion of the extrudate surface. This instability is referred to as sharkskin fracture, and has been discussed in relation to various aspects.

By this study, a laboratory scale 25 mm in diameter extruder is designed and produced for the processing of polyolefinic materials. Surface irregularities of the LDPE and HDPE have been investigated with an attached 25x1x26 mm profile die above the critical shear stress value. Effects of some fluouropolymeric additives as a PPA have been studied on polymer extrusion. Their efficiency for postponing surface irregularities has been investigated. A novel silicone based additive has been tested as a processing aid. Results have been observed by a close up camera and the changes in melt flow ratios by the addition of these additives have been investigated.



## **2. THEORY**

### **2.1. Extruder**

The extruders in the polymer industry come in many different designs. The main distinction between the various extruders is their mode of operation: continuous or discontinuous. The latter type extruder delivers polymer in an intermittent fashion and, therefore, is ideally suited for batch type processors, such as injection molding and blow molding. [2]

#### **2.1.1. Ram Extruder**

Ram or plunger extruders are simple in design, rugged, and discontinuous in their mode of operation. Ram extruders are essentially positive displacement devices and are able to generate very high pressures. Because of intermittent operation of ram extruders, they are ideally suited for cyclic processes, such as injection molding and blow molding. In fact, the early molding machines were almost exclusively equipped with ram extruders to supply the polymer melt to the mold. Certain limitations of the ram extruders have caused a switch to reciprocating screw extruders or combinations of the two. The types of the ram extruders are as follows;

- Single Ram Extruders
- Multi Ram extruders

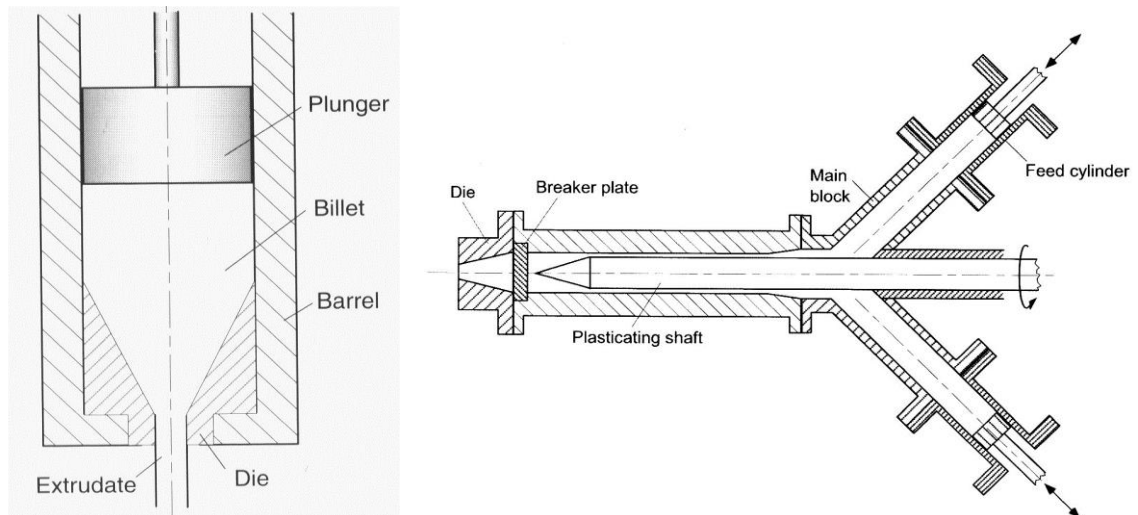


**Figure 2.1.** Single ram and twin ram extruder

### 2.1.2 Disk Extruders

There are a number of extruders, which do not utilize an Archimedean screw for transport of the material, but still fall in the class of continuous extruders. Sometimes these machines are referred to as screwless extruders. These machines employ some kind of disk or drum to extrude the material. Most of the disk extruders are based on viscous drag transport. One special disk extruder utilizes the elasticity of polymer melts to convey the material and to develop the necessary diehead pressure.

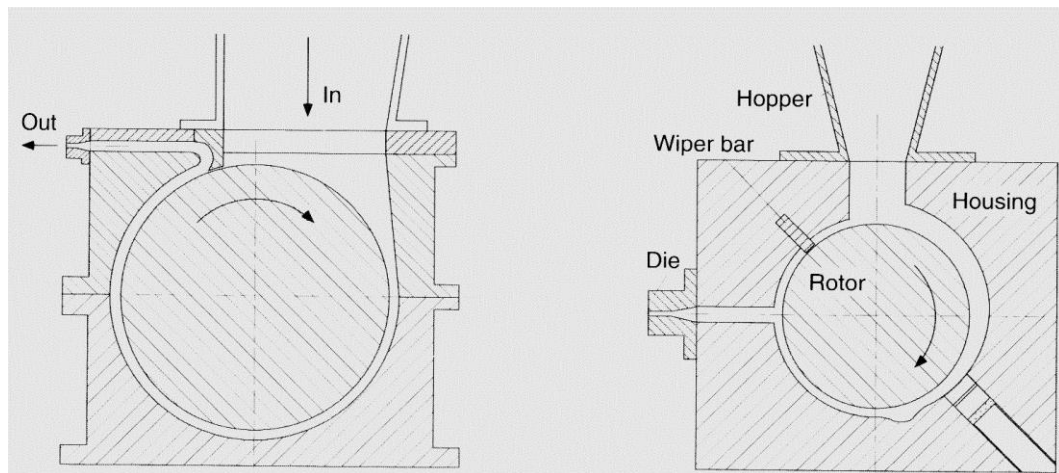


**Figure 2.2.** the drum disk extruder by Schmid & Kocher and Asco & Cosden

#### 2.1.2.1 Viscous Drag Disk Extruders

We can classify the Viscous Drag Disk Extruders as,

- Stepped Disk Extruder

- Drum Extruder
- Spiral Disk Extruder
- Diskpack Extruder

### 2.1.2.2 The Elastic Melt Extruder

The elastic melt extruder was developed in the late 1950s by Maxwell and Scalora. The extruder makes use of the viscoelastic, in particular the elastic, properties of polymer melts. In the elastic melt extruder, the polymer is sheared between two plates, one stationary and one rotating. As the polymer is sheared, normal stresses will generate a centripetal pumping action. Thus, the polymer can be extruded through the central opening in the stationary plate in a continuous fashion.

### 2.1.3. Screw Extruders

Screw extruders are divided into single screw and multi screw extruders.

#### 2.1.3.1 Single Screw Extruders

The single screw extruder is the most important type of extruder used in the polymer industry. Its key advantages are relatively low cost, straight forward design, ruggedness and reliability, and a favorable performance/cost ratio.

The extruder screw of a conventional plasticating extruder has three geometrically different sections. (Figure 1)

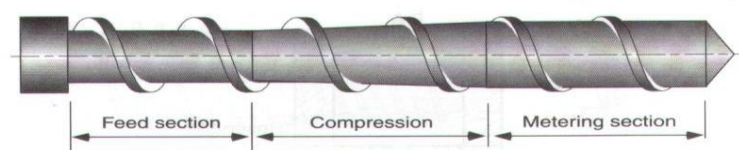


**Figure 2.3.** Schematic drawing of conventional plasticating single screw extruder

This geometry is also referred to as a 'single stage'. The single stage refers to the fact that the screw has only one compression section, even though the screw has three distinct geometrical sections. The first section (closest to the feed opening) generally has deep flights. The material in this section will be mostly in the solid state. This section is referred to as the feed section of the screw. The last section (closest to the die) usually has shallow flights. The material in this section will be mostly in the molten state. This screw section is referred to as the metering section or pump section. The third section connects the feed section and the metering section. This

section is called the transition section or compression section. In most cases, the depth of the screw channel (or the height of the screw flight) reduces in a linear fashion, going from the feed section towards the metering section, thus causing a compression of the material in the screw channel. This compression in many cases is essential to the proper functioning of the extruder.

The extruder is usually designated by the diameter of the extruder barrel. The standard extruder sizes are; 20, 25, 30, 35, 40, 50, 60, 90, 120, 150, 200, 250, 300, 350, 400, 450, 500 and 600 millimeters. Most extruders range in sizes from 25 to 150 millimeters. An additional designation often used is the length of the extruder generally expressed as length to diameter (L/D) ratio. Typical L/D ratios range from 20 to 30 with 24 being very common. Extruders used for the extraction of volatiles (vented extruders) can have an L/D ratio as high as 35 or 40 and sometimes even higher.

#### **2.1.3.2. Basic Operation**

The basic operation of a single screw extruder is rather straight forward. Material enters from the feed hoppers. Generally, the feed material flows by the gravity from the feed hopper down into the extruder barrel. Some materials do not flow easily in dry form. Special measures have to be taken to prevent hanging-up (bridging) of the material in the feed hopper.

As material falls down into the extruder barrel, it is suited in the annular space between the extruder screw and barrel, and is further bounded by the passive and active flanks of the screw flight: the screw channel, the barrel stationary, and the screw rotating. As a result, frictional forces will act on the material, both on the barrel as well as on the screw surface. These frictional forces are responsible for the forward transport of the material at least, as long as the material is in the solid state (below its melting point). As the material moves forward, it will heat up as a result of frictional heat generation and because of heat conducted from the barrel heaters. When the temperature of the material exceeds the melting point, a melt film will be formed at the barrel surface. This is where the solid conveying zone ends and the plasticizing zone starts. It should be noted that this point generally does not coincide with the start of the compression section. The boundaries of the functional zones will depend on polymer properties, machine geometry and operating conditions. Thus,

they can change as operating conditions change. However, the geometrical sections of the screw are determined by the design and will not change with the operating conditions. As the material moves forward, the amount of the solid material and each location will reduce as a result of melting. When all solid polymer has disappeared, the end of the plasticating zone has been reached and the melt conveying zone starts. In the melt conveying zone, the polymer melt is simply pumped to the die.

As the polymer flows through to die, it adapts the flow channel of the die. Thus, as the polymer leaves the die, its shape will more or less correspond to the cross sectional shape of the final portion of the die flow channel. Since the die exerts as a resistance to flow, a pressure is required to force the material through the die. This is generally referred to as the diehead pressure. Die pressure is determined by the shape of the die (particularly the flow channel), the temperature of the polymer melt, the flow rate through the die, and the rheological properties of the polymer melt. It is important to understand that the diehead pressure is caused by the die, and not by the extruder! The extruder simply has to generate sufficient pressure to force the material through to die. If the polymer, the throughput, the die, and the temperatures in the die are the same, then it does not make any difference whether the extruder is a gear pump, a single screw extruder, a twin screw extruder, etc.; the diehead pressure will be the same. Thus, the diehead pressure is caused by the die and by the flow process, taking place in the die flow channel.

#### **2.1.3.3. Vented Extruders**

Vented extruders are significantly different from non-vented extruders in design and in functional capabilities. A vented extruder is equipped with one or more openings (vent ports) in the extruder barrel, through which volatiles can escape. Thus, the vented extruder can extract volatiles from the polymer in a continuous fashion. This devolatilization adds a functional capability not present in non-vented extruders. Instead of the extraction of volatiles, one can use the vent port to add certain components to the polymer, such as additives, fillers, reactive components, etc. This clearly adds to the versatility of vented extruders, with the additional benefit that the extruder can be operated as a conventional non-vented extruder by simply plugging the vent port and, possibly, changing the screw geometry.

#### **2.1.3.4. Rubber Extruders**

Extruders for processing elastomers have been around longer than any other type of extruder. Industrial machines for rubber extrusion were built as early as the second half of the nineteenth century.

The first rubber extruders were built for hot feed extrusion. These machines are fed with warm material from a mill or other mixing device. Around 1950, machines were developed for cold feed extrusion. The advantages of cold feed extruders are: Less capital equipment cost, better control of stock temperature, reduced labor cost, capable of handling a wider variety of compounds.

Cold feed rubber extruders, nowadays, do not differ too much from thermoplastic extruders. Some of the differences are: Reduced length, heating and cooling, feed section, screw design.

There are several reasons for the reduced length. The viscosity of rubbers is generally very high compared to most thermoplastics; about an order of magnitude higher. Consequently, there is a substantial amount of heat generated in the extrusion process. The reduced length keeps the temperature build-up within limits. The specific energy requirement for rubbers is generally low, partly because they are usually extruded at relatively low temperatures (from 20 to 120 °C). This is another reason for the short extruder length. The length of the rubber extruder will depend on whether it is a cold or hot feed extruder. Hot feed rubber extruders are usually very short, about 5D (D=Diameter). Cold feed extruders range from 15 to 20 D. Vented cold feed extruders may be even longer than 20D.

#### **2.1.3.5 The Multi screw Extruder**

The screw extruders which have more than one screw are called as “Multi screw Extruders”.

#### **2.1.3.6. The Twin Screw Extruder**

A twin screw extruder is a machine with two Archimedean screws. There is a tremendous variety of twin screw extruders, with vast differences in design, principle of operation, and field of application. It is, therefore, difficult to make general comments about twin screw extruders. The differences between the various twin screw extruders are much larger than the differences between single screw extruders.

This is to be expected, since the twin screw construction substantially increases the number of design variables, such as direction of rotation, degree of intermeshing, etc. A classification of twin screw extruders is shown in table 2.1.

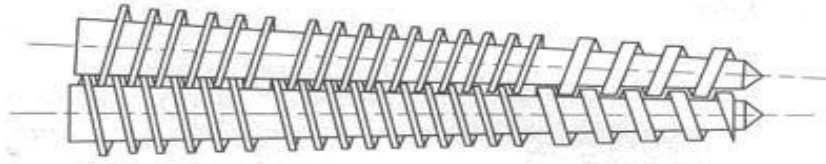


**Figure2. 4.** Counter rotating conical twin screw

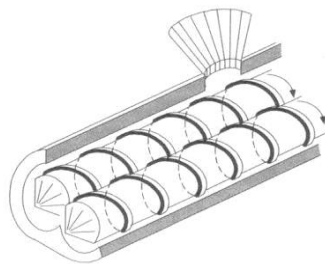


**Figure2.5.** Co-rotating parallel twin screw

**Table 2.1.** Types of twin screw extruders

Intermeshing extruders	Co-rotating extruders	Low speed extruders for profile extrusion High speed extruders for compounding
	Counter-rotating extruders	Conical extruders for profile extrusion Parallel extruders for profile extrusion High speed extruders for compounding
Non-intermeshing extruders	Counter-rotating extruders	Equal screw length Unequal screw length
	Co-rotating extruders	Not used in practice
	Co-axial extruders	Inner melt transport forward Inner melt transport rearward Inner solids transport rearward Inner plasticating with rearward transport

### **2.1.3.7. The Multi Screw Extruder with More Than Two Screws**

There are several types of extruders which incorporate more than two screws. One relatively well-known example is the planetary roller extruder.

This extruder looks similar to a single screw extruder. The feed section is, in fact, the same as on a standard single screw extruder. However, the mixing section of the extruder looks considerably different. In the planetary roller section of the extruder, six or more planetary screw, evenly spaced, revolve around the circumference of the main screw. This planetary barrel section results in effective devolatilization, heat exchange, and temperature control. Thus, heat-sensitive compounds can be processed with a minimum of degradation. For this reason, the planetary gear extruder is frequently used for extrusion/compounding of PVC formulations, both rigid and plasticized.

Gear pumps are also used in some extrusion operations at the end of a plasticating extruder, either single screw or twin screw. Strictly speaking, the gear pump is a closely intermeshing counter rotating twin screw extruder. However, since gear pumps are solely used to generate pressure, they are generally not referred to as an extruder.

## **2.2 Design of a Single Screw Extruder**

In order to design the polymer processing machines, rheology of the polymeric melt must be known.

### **2.2.1 Rheology of a Polymer Melts**

The transport properties of polymeric materials, which can distinguish them most from other materials, are their flow properties or rheological behavior. There are many differences between the flow properties of a polymeric fluid and typical low-molecular-weight fluids such as water, benzene, sulfuric acid, and other fluids that we classify as Newtonian. Newtonian fluids can be characterized by a single flow property called viscosity ( $\mu$ ) and by density ( $\rho$ ). Polymeric fluids, on the other hand, exhibit a viscosity function that depends on shear rate or shear stress, time-dependent rheological properties, viscoelastic behavior such as elastic recoil (memory),



additional normal stresses in shear flow, and an extensional viscosity not simply related to the shear viscosity, to name a few differences. [3]

Because of these vastly different rheological properties, polymeric fluids are known to exhibit flow behavior that cannot be accounted for merely through a single rheological parameter such as viscosity. Some of the differences in flow behavior include a nonlinear relation between pressure drop and volumetric flow rate for flow through a tube, swelling of the extrudate when emerging from a tube, the onset of a low Reynolds number flow instability called melt fracture gradual relaxation of stresses on cessation of flow, and the ability of the molecules to orient during flow.

The viscosities of typical polymer melts are nearly 1,000 Pa.s. Rheological properties of polymer melts can be obtained by rheometers, which measure viscosities and viscoelasticities of fluids and semi-solids (melts). The measuring ranges of rheometers change depending on the previously estimated viscosities of the materials. Methods commonly used for measuring the viscosity of polymer solutions and melts are listed in Table 2.2.

**Table 2.2.** Summary of methods for measuring viscosity

Method Used in Rheometers	Approximate useful viscosity range, Poises
Capillary pipette	$10^{-2} - 10^3$
Falling sphere	$1 - 10^5$
Capillary extrusion	$1 - 10^8$
Parallel plate	$10^4 - 10^9$
Falling coaxial cylinder	$10^5 - 10^{11}$

### 2.2.1.1 Viscous Behavior of Polymer Melt

When a Newtonian fluid is placed between the two plates as shown in Figure 2.6 , in which the top plate is moved to the right with constant velocity,  $v$ , the relation between force,  $F$ , divided by the area of the plates,  $A$ , and the velocity divided by the separation distance,  $H$ , is given as follows;

$$F/A = \mu V/H \quad (2.1)$$

The constant of proportionality,  $\mu$ , is called the viscosity of the fluid. The force,  $F$ , is the force required to keep the top plate moving at a constant velocity.

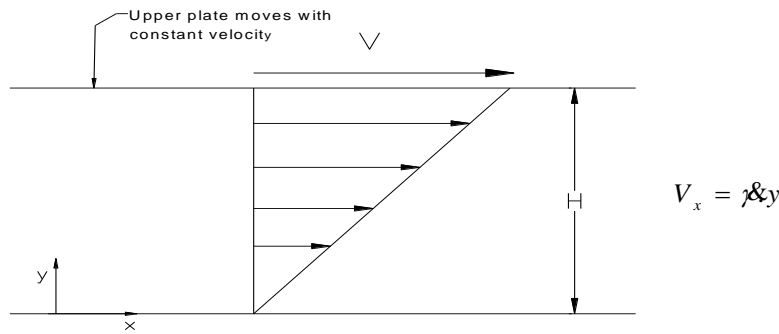


**Figure 2.6.** Steady simple shear flow with shear rate =  $V/b$

The force per unit area acting in the  $x$  direction on a fluid surface at a constant  $y$  by the fluid in the region of lesser is the shear stress,  $\tau_{yx}$ . Because the velocity of the fluid particles varies in a linear manner which respect to the  $y$  coordinate, it is clear that  $V/H = dv_x / dy$  as shown:

$$\lim_{\Delta y \rightarrow 0} \frac{\Delta V_x}{\Delta V_y} = \frac{V - 0}{H - 0} = \frac{V}{H} \quad (2.2)$$

This states that; the shear force per unit area is proportional to the negative of the local velocity gradient. This is known as Newton's law of viscosity.

The definition of  $\tau_{yx}$  can also be interpreted in another fashion.  $\tau_{yx}$  maybe considered as the viscous flux of  $x$  momentum in the  $y$  direction. The idea here is that the plate located at  $y = H$  transmits its  $x$  momentum to the layer below which in turn transmits momentum to the next layer. The momentum flux  $\tau_{yx}$ , is negative in this case as the momentum is transferred in the negative  $y$  direction. The sign

convention follows the ideas used for heat flux in that heat flows from hot to cold or in the direction of a negative temperature gradient. This also makes the law of viscosity fit with the ideas of diffusion in which matter flows in the direction of decreasing concentration.

Probably the most frequently used notation, however, is that found in mechanics in which material at a greater  $y$  exerts force in the  $x$  direction on a layer of fluid at a lesser  $y$ . The shear stress,  $\tau_{xy}$ , is then related to that used above as follows:

$$\tau_{yx} = -\tau_{xy} \quad (2.3)$$

$\tau_{xy}$  is then defined as the force per unit area acting in the  $x$  direction by fluid at  $y$  on a surface of lesser  $y$  with a unit outward normal in the  $+y$  direction. Flow behaviour of most thermoplastics does not follow Newton's law of viscosity.

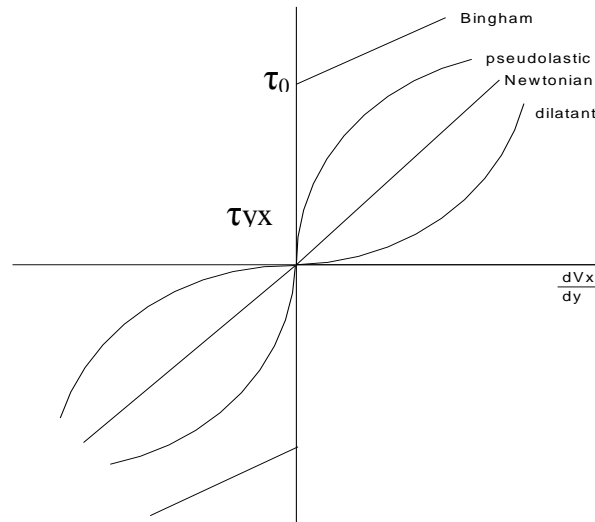


**Figure 2.7.** Viscous response of Non Newtonian fluids.

To quantitatively describe the viscous behavior of polymeric fluids, Newton's law of viscosity is generalized as follows;

$$\tau_{yx} = -\eta \frac{dV_x}{dy} \quad (2.4)$$

Where  $\eta$  can be expressed as a function of either  $dV_x / dy$  or  $\tau_{yx}$ . Some typical responses of polymeric fluids are shown in figure 2.7, where  $\tau_{yx}$  is plotted versus the velocity gradient. For a pseudoplastic fluid the slope of the line decreases with increasing magnitude of  $dV_x / dy$ , or in essence the viscosity decreases some polymeric fluids (in some cases polymer plants and field polymers) exhibit a yield stress, which is the stress that must be overcome before flow can occur. When flow

occurs, if the slope of the line is constant, then the fluid is referred to as a Bingham fluid. In many cases the fluid is still pseudoplastic once flow begins. Finally, in some cases the viscosity of the material increases with an increasing velocity gradient. The fluid is then referred to as dilatant.

Several flow equations are summarized in Table 2.3. for various models. Here  $\tau_0$  is the yield stress,  $\eta_0$  the viscosity at lower shear rates and  $\eta_\infty$  at the higher shear rates, and  $\alpha$  and  $n$  are constants.

**Table 2.3.** Flow models and equations

Model	Equation
Newtonian	$\tau = \eta \dot{\gamma}$
Bingham plastic	$\tau - \tau_0 = \eta \dot{\gamma}$
Power law	$\tau = \eta \dot{\gamma}^n$
Power law with yield value	$\tau - \tau_0 = \eta \dot{\gamma}^n$
Casson fluid	$\tau^{1/2} - \tau_0^{1/2} = \eta_\infty^{1/2} \dot{\gamma}^{1/2}$
Williamson	$\eta - \eta_\infty = \frac{(\eta_0 - \eta_\infty)}{1 + \tau / \tau_m}$
Cross	$\eta - \eta_\infty = \frac{(\eta_0 - \eta_\infty)}{1 + \alpha \dot{\gamma}^n}$

Much empiricism has been proposed to describe the steady state relation between  $\tau_{yx}$  and  $dV_x / dy$ , what we mention only a few that are most useful for polymeric fluids. The first is the Power-law of Ostwald-de Waele:

$$\eta = m \left| \frac{dV_x}{dy} \right|^{n-1} \quad (2.5)$$

This is a two-parameter model in which  $n$  describes the degree of deviation from Newtonian behavior.  $m$ , which has the units of  $\text{Pa.s}^n$ , is called the consistency. For  $n=1$  and  $m=\mu$ , this model predicts Newtonian fluid behavior. For  $n<1$ , the fluid is pseudoplastic and for  $n>1$  the fluid is dilatant. The Ellis model is a three-parameter model and is defined as:

$$\frac{\mu_0}{\mu} = 1 + \left( \frac{\tau_{yx}}{\tau_{1/2}} \right)^{x-1} \quad (2.6)$$

Here  $\eta_0$  is the zero shear viscosity, and  $\tau_{1/2}$  is the value of  $\tau_{yx}$  when  $\eta = 1/2\eta_0$ . Actually, most polymeric fluids exhibit a constant viscosity at low shear rates and then shear thin at higher shear rates. A model that is often used in numerical calculations, because it fits the full flow curve, is the Carreau model:

$$\frac{\eta - \eta_\infty}{\eta_0 - \eta_\infty} = \left[ 1 + (\lambda \dot{\gamma})^2 \right]^{\frac{n-1}{2}} \quad (2.7)$$

This model contains four parameters:  $\eta_0$ ,  $\eta_\infty$ ,  $\lambda$  and  $n$ .  $\eta_0$  is the zero shear viscosity just as before.  $\eta_\infty$  is the viscosity as the shear rate ( $\dot{\gamma}$ ) or  $dv_x/dy \rightarrow \infty$ , and for polymer melts this can be taken as zero.  $\lambda$  has units of seconds and approximately represents the reciprocal of the shear rate for the onset of shear thinning behavior.  $n$  represents the degree of shear thinning and is nearly the same as the value in the power-law model. As a number of polymeric fluids exhibit yield stresses, models that include these are the Bingham and Hershel-Bulkley models. The Bingham model is given as:

$$\begin{aligned} \eta &= \mu_0 + \left| \tau_0 \right| \left/ \frac{dV_x}{dV_y} \right. & \text{if } \left| \tau_{yx} \right| \geq \left| \tau_0 \right| \\ \eta &= \infty & \text{if } \left| \tau_{yx} \right| < \left| \tau_0 \right| \end{aligned} \quad (2.8)$$

Here  $\tau_0$  is the yield stress, and  $\mu_0$  is the slope of the line of  $\tau_{yx} - \tau_0$  versus  $dv_x/dy$ . The Hershel-Bulkley model is given as:

$$\eta = m' \left| \frac{dV_x}{dy} \right|^{n'-1} + \tau_0 \left/ \frac{dV_x}{dV_y} \right. \quad \text{if } \left| \tau_{yx} \right| \geq \tau_0 \quad (2.9)$$

Here  $m'$  and  $n'$  are power-law parameters determined from  $\tau_{yx} - \tau_0$  versus  $dv_x/dy$ . This model describes fluids that are pseudoplastic once flow starts.

### 2.2.1.2 Plasticating Single-Screw Extruders

Polymer solids (pellets or powder) enter the throat of the extruder. From this point they are transported through the extruder first by frictional drag and then by viscous drag. We first describe solids transport, then melting of the compacted solids, and finally the pumping of the melt.

### 2.2.1.3 Solids Transport

We consider the transport of particulate solids in a rectangular channel as shown in Fig.2.8. Our goal is to determine the mass flow rate and pressure rise as a function of the plate velocity and friction coefficient between the plate and pellets,  $f_{w1}$ . Although it would be desirable to somehow treat this situation in a manner similar to that for fluids in which we solve the equation of motion along with an appropriate constitutive equation, it is uncertain as to what constitutive equation best describes the flow of granular solids.

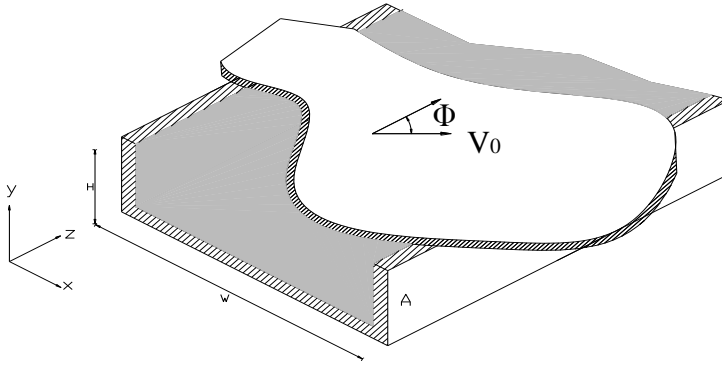


**Figure 2.8** Rectangular channel filled with granular solids with a plate moving at angle  $\Phi$  relative to the down channel direction.

For this reason we consider the particulate solids to be a plug of density,  $\rho_b$ , dragged along by the moving upper plate through Coulomb friction. The upper plate moves with a velocity,  $V^0$ , making an angle,  $\Phi$ , with the down-channel direction (i.e., the  $z$  direction). The tangential force exerted on the solid plug is in a direction that the

plate makes relative to the moving plug as shown in Fig.2.9. The velocity of the plate relative to the solid bed,  $v_r$ , is:

$$v_r = V_0 \sin \Phi \delta_x + V_0 \cos \Phi \delta_z - u \delta_{z'} \quad (2.10)$$

From Eq.2.10 we find that

$$\tan(\Phi + \Phi') = \frac{V_0 \sin \Phi}{V_0 \cos \Phi - u'} \quad (2.11)$$

Using a trigonometric identity for  $\tan(\Phi + \Phi')$  we obtain the following expression:

$$\tan \Phi' = \frac{u \sin \Phi}{v_0 - u \cos \Phi} \quad (2.12)$$

Equation 2.12 contains two unknowns,  $u$  and  $\Phi'$ , and hence an additional equation must be derived.

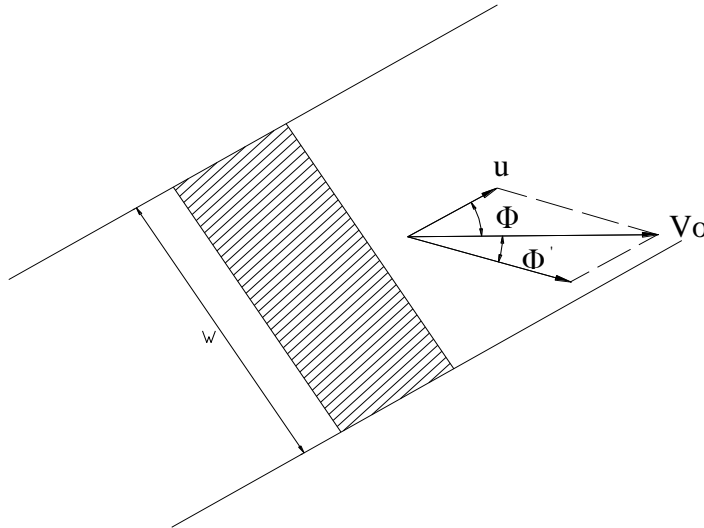


**Figure 2.9** Motion of the plate relative to motion of the solid bed. The plate moves at an angle  $\Phi'$  relative to solid bed.

The additional equation is obtained by performing a steady state force balance in the  $z$  direction on a differential element of thickness  $\Delta z$  (Fig. 2.9). Starting from the equation ;

$$P|_z WH - P|_{z+\Delta z} WH + KPWHf_{w1} \cos(\Phi + \Phi')\Delta z - KPWHf_{w2} \Delta z \quad (2.13)$$

On dividing through by the volume of the element and taking the limit as  $\Delta z$  goes to zero and integrated using the initial condition that at  $z=0$ ,  $P=P_0$ , to give;



$$P = P_0 \exp \left\{ \left[ Kf_{w.1} \cos (\Phi + \Phi') - Kf_{w.2} \right] z \right\} \quad (2.14)$$

The additional equation is obtained by performing a steady state for balance is the z direction on a differential element of thickness  $\Delta z$ . Starting from the equation;

$$P \left|_{z+\Delta z} \right. - P \left|_z \right. + Kf_{w.1} \cos (\Phi + \Phi') \Delta z - Kf_{w.2} \Delta z = 0 \quad (2.15)$$

The mass flow rate, G, is product of the plug velocity in the axial direction,  $V_{pl}$ ,  $\rho_b$  and of cross sectional area of the plug and is given by;

$$G = V_{pl} \rho_b \left[ \frac{\pi}{4} (D_b^2 - D_s^2) - \frac{eH}{\sin \Phi} \right] \quad (2.16)$$

where the second term on the right-hand side of the equation is where the flight cuts across the doughnut-shaped plug.  $\sin \Phi$  is the sine of the average helix angle  $D_b$  is the diameter of the barrel opening, and  $D_s = D_b - 2H$ .

$$V_{pl} = V_b \frac{\tan \Phi' \tan \Phi_b}{\tan \Phi' + \tan \Phi_b} \quad (2.17)$$

where  $V_b = \pi N D_b$  and N is the angular velocity of the screw in rev./second. We next substitute Eq.2.17 in to Eq.2.16 to obtain

$$G = \pi^2 N H D_b (D_b - H) \rho_b \frac{\tan \Phi' \tan \Phi_b}{\tan \Phi' + \tan \Phi_b} \left[ 1 - \frac{e}{\pi (D_b - H) \sin \Phi} \right] \quad (2.18)$$

Force and torque balances are then carried out to obtain the following expressions:

$$\cos \Phi' = K_s \sin \Phi' + M, \quad (2.19)$$

$$K_s = \frac{\bar{D}}{D_b} \frac{\sin \Phi + f_s \cos \Phi}{D_b \cos \Phi - f_s \sin \Phi} \quad (2.20)$$

The power input through the barrel is obtained from

$$P_w = \pi N D_b W_b Z_b f_b \cos \Phi' \frac{P_2 - P_1}{\ln (P_2 / P_1)} \quad (2.21)$$

The heat generated per unit of barrel surface is given by

$$q_b = f_b \pi N D_b \frac{\sin \Phi_b}{\sin (\Phi_b + \Phi')} - \frac{P_2 - P_1}{\ln (P_2 / P_1)} \quad (2.22)$$

Assuming that conduction occurs only in the y direction and with bulk flow in the z direction the equation of energy leads to the following differential equation for the temperature distribution:

$$\rho_b \bar{C}_{p,p} V_{pz} \frac{\delta T_p}{\delta z} = k_p \frac{\delta^2 T_p}{\delta y^2} \quad (2.23)$$

where  $T_p$  is the temperature in the plug and  $\bar{C}_{p,p}$  and  $k_p$  are the heat capacity and the thermal conductivity, respectively, of the plug. Equation 2.23 can be converted to the one dimensional transient heat conduction equation just as done in chapter 5 by replacing  $dz / V_{pz}$  by  $dt$ :

$$\frac{\delta T_p}{\delta t} = \alpha_p \frac{\delta^2 T_p}{\delta y^2} \quad (2.24)$$

where  $\alpha_p$  is the thermal diffusivity of the solid bed.  $V_{pz}$  is the velocity of the plug in the down- channel direction and is obtained from the equations derived for the isothermal case.

The following initial and boundary conditions are used;

Initial Cond. at  $t=0$   $T_p(y,t) = T_0$

Boundary Cond. 1 at  $y=H$   $T_p = T_b$

The additional boundary condition required to solve eq.2.24 comes from an energy balance at the interface between the barrel and the solid bed where it is assumed that the frictional heat is conducted away in to the barrel and the solid plug:

$$\text{Boundary Cond. 2 at } y=H \quad qb = -K_p \frac{\partial T_p}{\partial y} + K \frac{\partial T_b}{\partial y} \quad (2.25)$$

#### 2.2.1.4 Delay and Melting Zones

The basic model for the conversion of the solid bed to melt is due to Tadmor and is based on his observations of the state of material along the screw channel, according to which for most polymer systems a melt film first appears at the barrel surface as the result of heat generation due to friction and heat conducted from the heated barrel. Once the melt film forms, the conveying mechanism changes at the barrel surface where viscous drag is now dominant, but frictional drag is still important at

the root of the screw and the flights. The thickness of the melt film continues to increase as the plug proceeds down the channel until it attains a value of several times the flight clearance. At this point, the melt film thickness stays nearly constant and the melt is scraped off and accumulated at the pushing flight. The axial distance from where the melt film first appears until melt begins to accumulate at the pushing flight is referred to as the delay zone.

The goal of a model of the melting section is to determine the solid bed width,  $X$ , as a function of the down- channel distance,  $z$ .

The solid bed is assumed to move as a plug with down-channel velocity of  $V_{sz}$  where;

$$V_{sz} = G / (\rho_s HW) \quad (2.26)$$

For the melt film, the equations of motion and energy are

$$\frac{\delta \tau_{yx}}{\delta y} = 0 \quad (2.27)$$

$$\frac{\delta \tau_{yz}}{\delta y} = 0 \quad (2.28)$$

$$\rho_s \bar{C}_p V_x \frac{\delta T}{\delta x} = +k \frac{\delta^2 T}{\delta y^2} + k \frac{\delta^2 T}{\delta x^2} - \tau_{yx} \frac{\delta v_x}{\delta y} - \tau_{yz} \frac{\delta v_z}{\delta y} \quad (2.29)$$

Because of the homogeneous nature of Equations 2.27, and 2.28 the viscosity function drops out, and the velocity field becomes;

$$v_x = \left( \frac{V_{bx}}{\delta} \right) y \quad (2.30)$$

$$v_z = \left( \frac{V_{bz} - V_{sz}}{\delta} \right) y + V_{sz} \quad (2.31)$$

The temperature distribution in the solid bed is determined next. Assuming that  $T_s = T_s(y)$ , then the energy equation becomes

$$\rho_s \bar{C}_{ps} V_{sy} \frac{\delta T_s}{\delta y} = k \frac{\delta^2 T_s}{\delta y^2} \quad (2.32)$$

For a tapered channel of constant taper, which is usually the case, we write as;

$$\frac{d(HX)}{dH} = \frac{\Phi \sqrt{X}}{A \rho_s V_{sz}} \quad (2.33)$$

$$\Phi = \left\{ \frac{V_{bx} \rho_m \left[ k_m (T_b - T_m) + (\mu / 2) V_j^2 \right]}{2(\bar{C} (T_m - T_0) + \Delta \bar{H}_f)} \right\} \quad (2.34)$$

$$A = - \frac{dH}{dz} \quad (2.35)$$

Equation 2.33 can be integrated to give;

$$\frac{X_2}{W} = \frac{X_1}{W} \left[ \frac{\Psi}{A} - \left( \frac{\Psi}{A} - 1 \right) \sqrt{\frac{H_1}{H_2}} \right]^2 \quad (2.36)$$

Where X2 and X1 are the widths of the solid bed at down-channel locations corresponding to H2 and H1, respectively.

Equation 2.36 represents the basic equation for the melting model. The total length of melting for a tapered channel is;

$$z_T = \frac{H}{\Psi} \left( 2 - \frac{A}{\Psi} \right) \quad (2.37)$$

### 2.2.1.5 Metering zones

The fully melted polymer now enters the third zone of the extruder where it is pressurized. The buildup of pressure is required in order to pump the melt through the die at the end of the extruder. The pressurization of the melt is based on a viscous drag mechanism. We illustrate how viscous drag can lead to pressurization of the melt. We also present the isothermal Newtonian case where a analytical solution is possible.

For the shear stress for a Newtonian fluid, the equation of motion becomes;

$$\mu \frac{d^2 V_z}{dy^2} - \frac{dp}{dz} = 0 \quad (2.38)$$

This equation is solved by the following boundary conditions;

Boundary Condition 1 at y=0  $V_z = 0$

Boundary Condition 2 at  $y=0$   $V_z = V_0$

After integrating Eq. 2.38 and using the boundary conditions;

$$v_z = (H^2 / 2\mu) \left( \frac{dp}{dz} \right) \left[ \left( \frac{y}{H} \right)^2 - \frac{y}{H} \right] + \frac{V_0 y}{H} \quad (2.39)$$

By integrating over the cross-sectional area to obtain the volumetric flow rate:

$$Q = \frac{V_0 WH}{2} - \frac{dp}{dz} \left( \frac{WH^3}{12\mu} \right) \quad (2.40)$$

$Q$  is seen to consist of two terms: the first is called the drag flow,  $Q_d$ , and the second is referred to as the pressure flow,  $Q_p$ . When there is no pressure buildup, then the transport is due entirely to the drag flow term.

If  $W/H > 10$ , then we can simplify matters by making the following postulates for the velocity field:

$$v_z = v_z(y) \quad v_x = v_x(y) \quad (2.41)$$

Using these postulates, the equations of motion and energy become, respectively:

$$0 = -\frac{\delta p}{\delta x} - \frac{\delta \tau_{yx}}{\delta y} \quad (2.42)$$

$$0 = -\frac{\delta p}{\delta z} - \frac{\delta \tau_{yz}}{\delta y} \quad (2.43)$$

$$\rho C_p v_z \frac{\delta T}{\delta z} = k \frac{\delta^2 T}{\delta y^2} - \tau_{xy} \frac{\delta v_x}{\delta y} - \tau_{yz} \frac{\delta v_z}{\delta y} \quad (2.44)$$

Using the GNF model, the shear stress components are given by:

$$\tau_{yx} = -\eta(\lambda T) \frac{\delta v_x}{\delta y} \quad (2.45)$$

$$\tau_{yz} = -\eta(\lambda T) \frac{\delta v_z}{\delta y} \quad (2.46)$$

Where  $\lambda$  is given by:

$$\gamma = \sqrt{\left(\frac{\delta v_x}{\delta y}\right)^2 + \left(\frac{\delta v_z}{\delta y}\right)^2} \quad (2.47)$$

The volumetric flow rate is obtained by integrating the velocity field over the cross-sectional area and is:

$$\frac{Q}{WHV_{bz}} = \left(\frac{GH^{n+1}}{mV_{bz}^n}\right)^s \left[ -\frac{\beta^{s+2}}{s+1} - \frac{(1-\beta)^{s+2}}{s+2} \right] + (1-\beta) \quad (2.48)$$

For a Newtonian fluid following expression for  $u_x$  and  $u_z$  can be written:

$$u_x = -\zeta + \zeta(\zeta - 1) \left( GH^2 / 2\mu V_{bx} \right) \quad (2.49)$$

$$u_z = \zeta - 3\zeta(1 - \zeta) \left( H^2 G / 6\mu V_{bz} \right) \quad (2.50)$$

The volumetric flow rate is obtained by integrating Equation 2.50 over the cross-sectional area of the channel and is:

$$Q = \frac{V_{bz} WH}{2} - \left( \frac{\delta p}{\delta z} \right) \frac{WH^3}{12\mu} \quad (2.51)$$

This is the screw characteristic for the Newtonian case, and, as shown in the simple one-dimensional flat plate model, it consists of drag and pressure flow terms. The ratio of pressure to drag flow rates (sometimes called the throttle ratio) is:

$$Q_p / Q_d = - \left( \frac{\delta p}{\delta z} \right) \frac{H^2}{6\mu V_{bz}} \quad (2.52)$$

The pressure buildup along the axial direction of the extruder is due to the resistance offered by the die and other elements such as connectors and filtration systems. Hence, the operation of the extruder is directly affected by the design of the die and connecting elements. To illustrate this, we again consider the fluid to be Newtonian, and we consider only the metering section of the extruder. Furthermore, we assume that the die is a simple capillary, and we neglect any pressure losses due to constructions or expansions in the system. Using Eq.2.51 we write the screw characteristic as:

$$Q_s = \frac{1}{2} \pi D_b^3 N \cos \Phi WH - \left( \frac{\Delta P_s}{L_h} \right) \frac{WH^3 \sin \Phi}{12\mu} \quad (2.53)$$

Where  $Q_s$  is the volumetric flow rate in the extruder,  $\Delta P_s$  is the pressure rise in the extruder,  $L_b$  is the extruder length, and  $\Phi$  is the average helix angle. Because of some side effects and empirical approach some practically used equations gives more realistic results. For an approximate result for mass capacity of a single screw extruder, following formula can be used;

$$Q_m = 0.079 D^2 H N \rho \quad (2.54)$$

Where the  $Q_m$  is the mass flow rate,  $D$  is the diameter of the screw  $H$  is the depth of the metering section flight,  $N$  is the rotational speed of the screw, and  $\rho$  is the melt density of the material.

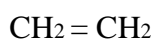
## 2.3 Polyolefines

Polyolefines is the collective name for polyethylene (PE) and polypropylene (PP) - among the most widely used plastics today. They account for more than half of total plastics consumption in the developed world [4]

### 2.3.1 Polyethylenes and ethylene copolymers

In this section different types of Polyethylene (PE) which are in general use will be explained. Some special types of PE which can be distinguished among others by some specific properties will be explained under subtitles. PE is a semi crystalline, light weight thermoplastic. It is produced by polymerizing ethylene gas ( $C_2H_4$ ) in the presence of a catalyst under controlled conditions of temperature and pressure. Small percentages of comonomers sometimes are incorporated. Polyethylene, in it is various forms, finds use in such diverse products as coatings on milk and food cartons, adhesive and moisture barriers in multilayered structures, clear thin films for produce and stretch /cling wrap, strong films for merchandise and grocery bags, milk and water bottles, gas and water pipe, house wares, caps and closures, coatings on communication and power cable, drums, and industrial containers and etc.

Polyethylene is formed when the proper combination of catalyst, temperature, and pressure open the ethylene



Double bond and start a chain reaction that links ethylene molecules together. The basic unit is the saturated moiety.



The structure of the molecule can be altered by the catalyst and reaction conditions used. Relatively low pressures and temperatures combined with supported transition metal catalysts are used to produce rather linear molecules, which result in a high density product. The density is lowered and the properties altered by incorporating alpha-olefin comonomers ( e.g., butane or hexane) with the ethylene. Higher pressures and temperatures combined with peroxide-type catalysts produce a relatively highly branched molecule, which results in a low density product. The properties of the material can be modified by the incorporation of polar comonomers (for example, vinyl acetate) into the ethylene chain.

A third type of polyethylene, linear low density polyethylene, can be produced using either the high pressure or the low pressure approach and alpha-olefin comonomers such as butane, hexane, octane, etc.

A fourth type of polyethylene, high-molecular-weight low density polyethylene exhibits the high strength and good draw-down of LLDPE as well as the optical properties of high-clarity conventional LDPE.

ASTM defines polyethylene types in terms of density as follows:

**Table 2.4** Classification of the Polyethylenes

<b>Type</b>	<b>Density, g./cc.</b>
I.	0.910 to 0.925
II.	0.926 to 0.940
III.	0.941 to 0.959
IV.	0.960 and higher

I and II are referred to as low-density polyethylene and medium density polyethylene respectively. Type III is copolymer high density PE and Type IV is homo-polymer high density polyethylene. Melt blends of LDPE and HDPE can be made to produce MDPE. Alternatively, MDPE can be synthesized directly as LLDPE.

As density increases, barrier properties, hardness, abrasion resistance, tensile strength, rigidity, heat resistance, chemical resistance, and surface gloss also



increase. Decreasing density leads to increased toughness, stress-crack resistances, clarity, flexibility, and elongation. It also will reduce creep and mold shrinkage.

In addition to density, molecular weight (MW) and Molecular weight distribution (MWD) play an important role in the properties of polyethylene. The melt index (MI) usually is expressed in terms of g./10 min. Generally, as average MW increases, MI decreases. Increasing MI improves clarity, surface gloss, and mold shrinkage. It leads to increased draw-down in blown film and extrusion coating applications. Decreasing MI improves creep resistance, heat resistance, toughness, melt strength, stress- crack resistance, and neck-in characteristics (in extrusion coating). In general, low MI resins are used for blow molding, where good melt strength in the parison is required. Low MI resins are used in injection molding of thick parts, while high MI resins are needed for long, thin, injection molded parts. Extrusion coating requires higher MIs for draw-down. Blown film uses lower MIs for better strength.

Two resins can have the same MI (avg. MW) but different MWD. Narrower MWD will give better impact strength and low temperature properties to a product, but the resin will be somewhat more difficult to process. A resin with broader MWD will exhibit greater shear sensitivity. This means that at higher shear conditions, as in an extruder, the resin will have lower viscosity and be easier to process. And at low shear conditions, after the resin exits the die, the resin will have a higher viscosity for better melt strength. Various types of PE is generally used with almost all kinds of application such as blown film, cast film, extruded sheet, extrusion coating, wire and cable coating, pipe and profile extrusion, blow molding, injection molding, injection blow molding, rotational molding, powder molding, foam molding and co-extrusion.

#### **2.3.1.1 LLDPE (Linear Low Density Polyethylene)**

Linear Low Density Polyethylene (LLDPE) is often replacing conventional Low Density Polyethylene (LDPE) because of combination of favorable economics and product performance characteristic.

LDPE is produced primarily at low pressure and temperatures either in gas phase fluidized bed reactors or liquid phase solution process reactors. In contrast, LDPE is produced at very high pressures and temperatures either in autoclaves or tubular reactors.

LDPE is produced by the copolymerization of ethylene with various alpha olefins in the presence of suitable catalyst. Polymer properties such as molecular weight, molecular weight distribution, and density (crystallinity) are controlled through catalyst selection and regulation of reactor condition. The stress crack resistance of LLDPE is considerably higher than that of LDPE having the same melt index and density. Similar comparisons can be made by puncture resistance, tensile elongation, tensile strength and high temperature toughness. LLDPE allows producers to make either a stronger product at the same gage or an equivalent product at a reduced gage.

#### **2.3.1.2 Very Low Density Polyethylene**

Very Low Density Polyethylene (VLDPE) is a new class of Linear Polyethylene Copolymers with densities ranging between 0,890 and 0,915 g. / cc. VLDPE offers the flexibility previously available only in generally lower-strength materials, such as Ethylene Vinyl Acetate (EVA), Ethylene-Ethyl-Acrylate (EEA), and plasticized PVC, together with the toughness and broader operating temperature range of linear low density polyethylene. VLDPE can be readily processed on existing polyethylene extrusion, injection molding, and blow molding machinery.

#### **2.3.1.3 HMW High Density Polyethylene**

High-molecular-weight high density polyethylene is defined as a linear homopolymer or copolymer with typical weight average molecular weight (Mw) in the range of approximately 200,000 to 500,000. HMW-HDPE is characterized by superior stress-crack resistance, impact strength, tensile strength, and good long-term performance in critical environmental applications. The combination of high molecular weight and high density provides good stiffness characteristics together with above-average abrasion resistance and chemical resistance.

#### **2.3.1.4 Ethylene-methyl-acrylate**

Ethylene-methyl-acrylate (EMA) is one of the most thermally stable of the high-pressure alpha olefin copolymers. EMA alone or in blends has found many applications in film, extrusion coating, sheet extrusion, blow molding, tubing, profile extrusion, and co-extrusion areas. It also makes a good master-batch base resin as it

can be filled to more than 60% without loss of its elastomeric characteristics and it is compatible with all the polyolefin resins.

#### **2.3.1.5 Ethylene-ethyl-acrylate**

Ethylene-ethyl-acrylate (EEA) copolymers are low-modulus members of the polyethylene family. They resemble PE in appearance but have the flexibility of plasticized vinyls without the thermal instability and plasticizer migration problems which are often associated with PVC.

#### **2.3.1.6 Ethylene-vinyl-acetate**

Ethylene-vinyl-acetate (EVA) copolymers are derived from basic low density polyethylene (LDPE) technology. EVA describes a family of thermoplastic polymers ranging from 5 to 50 % by weight of vinyl acetate incorporated into an ethylene chain. Copolymers containing less than 5 % vinyl acetate are defined as PE or modified PE; above 50 % vinyl acetate they are considered vinyl acetate-ethylene (VAE) copolymers. Addition of vinyl acetate reduces polymer crystallinity, which increases the flexibility and reduces the hardness.

#### **2.3.1.7 UHMW Polyethylene**

Ultrahigh-molecular-weight polyethylene (UHMWPE) is defined by ASTM as PE with molecular weight over 3 million (weight average). Although this resin is chemically similar to HDPE, its very long, substantially linear chains provide great impact strength, abrasion resistance, toughness, and freedom from stress-cracking in addition to the typical PE characteristics of chemical inertness, lubricity, and electrical resistance. This very high molecular weight provides an intractable polymer difficult to process by standard molding and extrusion techniques. Compression molding of sheets and ram extrusion of profiles are the standard manufacturing techniques.

### **2.3.2 Polypropylene**

The key properties of polypropylene are its low specific gravity, high heat resistance, stiffness, and chemical resistance.

PP manufacturing process involves the polymerization of propylene monomer with an organometallic catalyst of the Ziegler-Natta type. Key to many of the desirable

properties of PP is its crystallinity, which in term is dependent upon the stereo specific arrangement of methyl groups along the polymer backbone. Among its characteristic properties, PP has a specific gravity of 0.90 to 0.91 making it the lightest among the major plastics. The melting point of PP homopolymer is 168° C., and PP has been found to be suitable for continuous low stress structural applications up to 135° C. The homopolymer has a flexural modulus of 190 to 240M p.s.i., making PP the stiffest of the polyolefines. PP parts also exhibit good flex life, such that thin sections are applicable for use as integral hinges. Chemical resistance extends to nonoxidizing inorganics, detergents, low boiling hydrocarbons, and alcohols. The tertiary hydrogens present on the polymer backbone are subject to scission by free radical sources. Hence, PP is normally stabilized to prevent oxidative degradation during processing and normal end-use conditions.

Homopolymers are used for about 80% of PP's applications, with melt flows ranging from less than 1 to greater than 100. Lower-flow grades are used for sheet, film, and general purpose extrusion, while higher flows are employed for injection molding and fine-denier fibers.

Random copolymers are made by introducing small amounts of ethylene (normally 2 to 5%) into the polymerization reactor. This results in a product with much improved clarity and somewhat improved toughness at the expense of stiffness. A drawback of homopolymer PP is its poor impact resistance at low temperatures. One way to improve its impact properties is to blend in an elastomer, such as EP rubber up to 25%. Another approach has been to use 2 or more polymerization reactors in sequence, with ethylene introduced into the latter reactors. This results in an in situ copolymer with significantly improved impact characteristics, again at some sacrifice in stiffness. By blending elastomers with such copolymers, one can achieve even higher impact performance.

PP can be compounded with a variety of inorganic fillers such as talc, calcium carbonate, mica, and glass fiber to improve selected mechanical and thermal properties. Ignition-retardant formulations also are available, as are compounds with other polymers. Blends of PP with about 40% EP rubber are known as TPOs, and exhibit both thermoplastic and elastomeric properties.

## 2.4 Extrudate flow instabilities

Polymer extrudate flow exhibits instabilities under sufficiently high stress. In the case of linear polymers such as high-density polyethylenes, the first appearance of instability is periodic small-amplitude distortion of the extrudate surface. This instability is referred to as sharkskin fracture, and has been discussed in relation to various aspects.

In the case of extrusion through a capillary die, at sufficiently low extrusion rates, the polymer is smooth as it exits the die. At progressively higher extrusion rates, a series of flow instabilities occurs. The first instability that may occur is known as sharkskin or sharkskin melt fracture and is characterized by surface roughness. At higher extrusion rates, one observes an oscillating stick–slip transition, followed at higher rates by gross melt fracture in which the polymer is extruded in an extremely irregular fashion. The occurrence of the instabilities is dependent on many factors including polymer chemistry, architecture, molecular weight and distribution, and polymer/wall surface interactions.

When linear polyethylenes of high molecular weight and narrow molecular weight distribution are extruded through a narrow die gap, it is found that smooth extrudates can only be obtained at relatively low shear rates. This limits maximum production rates in commercial applications, such as in blown and cast film and in wire coating. During extrusion, at a critical wall shear stress greater than about 0.1 MPa, fine-scale surface irregularities appear, commonly known as sharkskin. These irregularities increase in severity up to a second critical wall shear stress of about 0.4 MPa, where polymer flow becomes markedly unsteady and gross extrudate distortion, or gross melt fracture, appears. [5].

The slip velocity increases uniformly with increasing shear stress up to the second critical shear stress, at which polymer flow becomes unsteady.

The appearance of wall slip and sharkskin at approximately the same critical wall shear stress suggests that slip may be the cause of sharkskin melt fracture. However, observations of the effects of processing aids on the appearance of both sharkskin and on slip demonstrate that other factors, such as acceleration and stretching in the surface layer of the melt as it leaves the die must also be important. For example, if as little as 0.05% by weight of a vinylidene fluoride/hexafluoropropylene (VFzA-

IFP) fluoroelastomer (ASTM designation FKM) is added to a linear low-density polyethylene, it is found that sharkskin is completely eliminated at all extrusion rates up to the second critical wall shear stress (0.4 MPa), at which value gross melt fracture again.

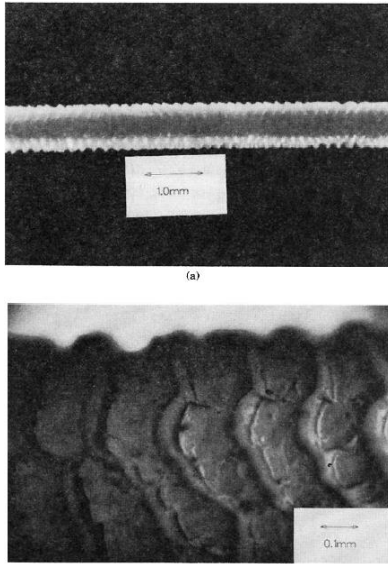


**Figure 2.10** LLDPE extrudate displaying sharkskin  $V/D= 985$

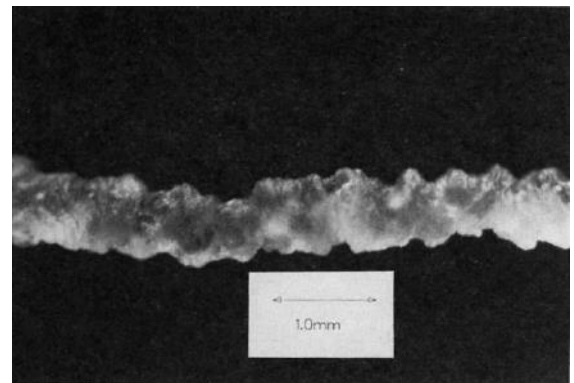


**Figure 2.11** LLDPE extrudate displaying wavy fracture  $8 V/D= 6155$

Since melt fracture can be eliminated and extrusion rates significantly increased by enhancing slip at the die wall, through the use of a fluoropolymer processing aid, it is important commercially to understand and to control the factors which influence both the onset and the magnitude of slip. These factors include the type of polymer being processed, its molecular weight and molecular weight distribution, whether the polymer is linear or branched, temperature and pressure during processing, nature of the die surface and the nature of the fluoropolymer processing aid. The purpose of this study was to understand the influence that each of these factors has on the ability of a variety of fluoropolymers to act as processing aids by enhancing slip.

Tordella (1958) [6] studied general fracture behaviors of low density polyethylene (LDPE), polymethylmethacrylate (PMMA), and polytetrafluoro-ethylene (PTFE) in extrusion, but the sharkskin surface fracture was not clearly differentiated from other

flow instabilities such as elastic turbulence. Nevertheless, the entrance instability has continued to be connected with the sharkskin melt fracture [7, 8]. Howell and Benbow (1962) [9] proposed that the sharkskin melt fracture originated at the die exit. They observed that the sharkskin melt fracture was caused by the body of extrudate moving away from a relatively stationary bank of polymer held near the die plane. They suggested that a type of stick-slip effect between polymer melt and the metal might be responsible for the formation of sharkskin. Petrie and Denn [5] made a careful, objective assessment of all the available evidences, both for and against slip, and concluded, “At present it is an open question as far as linear polymers are concerned. It is almost certain that slip is negligible for branched polymers.” The literature suggests that surface melt fracture is a die exit phenomenon and occurs as a consequence of high local stresses as the viscoelastic melt parts company with the die.

The irregularities are generally classified into two groups:

Surface irregularities which often occur under constant shear stress regardless of extrusion temperature and gross irregularities melt fracture, which occur at unsteady flow conditions.

By studying the sharkskin phenomena of LLDPE, Kurtz (1984) [10] also hypothesized that a fast stretching due to the velocity profile discontinuity at the die exit distorts the extrudate surface. He found that the sharkskin melt fracture of several LLDPEs occurred at a critical shear stress of approximately 0.1 MPa, which was associated with a slope change in the stress-rate flow curve. On considering the flow-curve changes and the sharkskin phenomenon in LLDPE extrusion, Ramamurthy (1986) [11], Kalika and Denn (1987) [12], and Person and Denn (1997) [13] addressed the interfacial effects between die walls and LLDPE melt.

Wall slip may be another important factor in sharkskin fracture. Ramamurthy (1986) found that the appearance of sharkskin is influenced by the die-lip material, and this finding triggered several studies focusing on the relationship between wall slip and extrudate instability. The influence of slippery surfaces on the extrudate instability was reviewed by Piau et al. [14,15].

Hatzikiriakos and Dealy (1991, 1992) [16, 17] carefully studied the wall slip of linear polyethylene by using both a sliding plate and a capillary rheometer. Thus the stress

of 0.1 MPa has been viewed as the critical number for both onset of sharkskin and wall slip for linear polyethylene. This apparently compelling correlation between the sharkskin and the wall slip at the critical stress has attracted substantial attention, Beaufils et al., 1989 [18]; Piau et al., 1990 [19]. Influence of upstream instabilities and wall slip on melt fracture and sharkskin phenomena during silicones extrusion through orifice dies were investigated [20]. Hatzikiriakos and Dealy, 1993 [21]; El Kissi and Piau, 1998[22]

Effects of surface properties on polymer melt slip and extrusion defects. *J Non-Newtonian Fluid Mech* 52:249–261); Hatzikiriakos et al., 1995 [23]; (La Mantia et al. 1995) [24], Fraser and Herdle (1987) [25] studied an organosilicon chemical as a processing aid for extrusion grade polyolefines (Schumacher 1986) [26]. They demonstrated that this chemical at trace concentration levels 500–1000 ppm has the ability to aid the extrusion of PE, to reduce the extruder power requirement, and to eliminate melt fracture. Fluoroelastomers, copolymers of vinylidene fluoride and hexafluoropropylene, have been extensively used as processing aids in the polyolefin processing Rudin et al.(1985a,b) [27,28]; Rudin et al. (1986) [29]; De Smedt and Nam (1987) [30], Klein (1987) [31]; Johnson et al. (1988) [32]; The presence of a fluoroelastomer, either as a slip promoter or an adhesion promoter, causes a decrease of the critical shear stress for the onset of slip, consequently, improving the extrudate appearance. It is also shown that; addition of the fluoroelastomers at 500–1000 ppm concentration levels may be able to eliminate melt fracture, however, it appears that higher concentrations are required to minimize sharkskin.

In comparison to the die land, the die exit plays a critical role in wall slip, because of the high local shear of this area. Moreover, polymer chains experience high stretching as a result of rapid flow acceleration. This polymer stretching on the surface was proposed by Cogswell (1977) [33] as the cause of extrudate instabilities. Stretching beyond than the polymer stretching strength causes cracks to open on the extrudate surface, and sharkskin roughness appears. Wang et al. (1996) [34] Suggested that the sharkskin periodicity corresponds to the oscillation of polymer chains between entangled and disentangled states. Inn et al. (1998) [35] and Migler et al. (2002) [36] Investigated the kinetics of sharkskin instability by employing video microscopy in the vicinity of the die exit. In these observations, the rough element of sharkskin is often referred to as a ridge rather than as a crack. The term crack



suggests tearing of the extrudate surface, whereas the term ridge emphasizes expansion of the surface as the die swells. This difference in the appearance of the extrudate is also thought to depend on the roughness pitch and the degree of swelling; however, the instability mechanism that produces the cycle of cracks or ridges remain uncertain. In order to reveal this instability in the vicinity of the exit, simultaneous measurements both inside and outside the die are crucial.

By this study, the effects of some fluoropolymeric additives as a PPA is studied on polymer extrusion. A novel silicone based additive will be tested as a processing aid. Results are observed by a close up camera and melt flow ratios will be measured. How the melt index was affected by the addition of these additives will be investigated.

### 3. EXPERIMENTAL

Experimental studies were done in two main subjects; preparation of a lab scale extruder machine and investigation of the periodic surface distortions in extrusion of polyolefines and usage of novel processing aids to overcome these instabilities.

#### 3.1. Preparation of the laboratory extruder

In order to make the surface distortion experiments; we prepared an extruder as a part of this study. We intended to design the extruder as a universal laboratory extruder which can be run with various types, small quantity experiment samples. Because of some construction limitations extruder was designed as a 25 mm in diameter, 25 turns long extruder to work with minimum 200 g sample. Even it can work with 200 g sample; 500 g. samples are generally required to have satisfactory results. Design of extruder screw and barrel and the constructional design of the extruder were made as a part of this study.

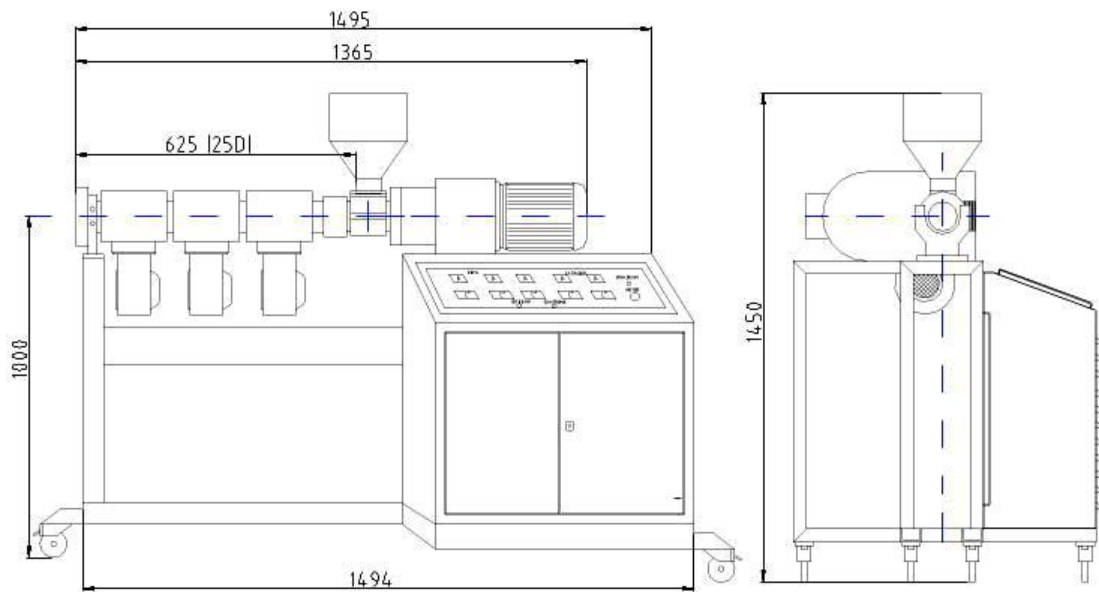


**Figure 3.1.** Constructional drawing of the extruder

### 3.1.1. Design of screw and barrel

Since we intended to prepare a universal extruder which can be used for various polymers, we chose the processing length of the screw L/D (Length/Diameter) of 25 which is the optimum length for single screw extruders. Compression ratio (ratio of metering section flight depth/feeding section flight depth) of 1/ 2,2 was applied. The required capacity for the extruder was small as much as possible to run it with minimum sample quantities. The calculated specific capacity (capacity per round per hour) for LDPE for the chosen design related to formula 2.54 is 63g. This is a suitable quantity to run the extruder for experiments.

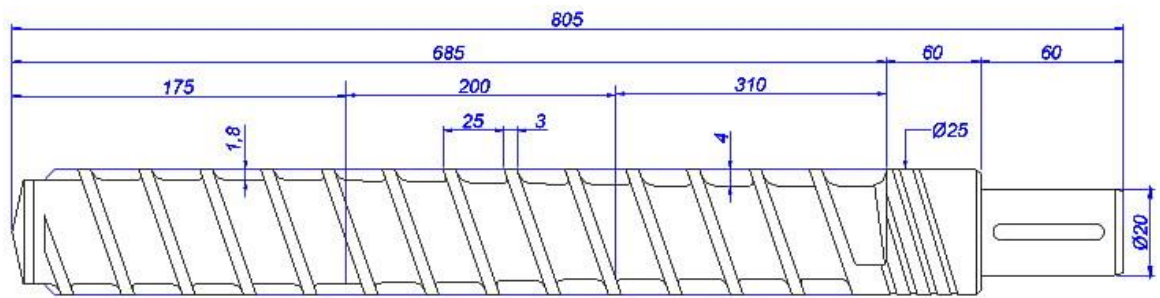


**Figure 3.2.** Design of the screw

### 3.1.2. Material used in preparation of screw and barrel

The steel type used for the production of screw and barrel was chosen related to the needs for the running conditions of screw and barrel. In order to have better results against abrasion, corrosion or mechanical resistance, DIN 1.2891 nitriding steel was chosen with the support of gas nitriding.

### 3.1.3. The main components of the extruder

Main components of the extruder, except screw and barrel can be categorized in 5 titles.

#### 3.1.3.1 Motor

To supply the power for the movement of the screw, a 3 KW, 1450 r.p.m., AC electric motor was used which was made by Gamak Company.

### 3.1.3.2 Reduction gear box

A reduction gear box was used to deliver AC motor torque to the screw by a reduced turning speed of 97 r.p.m. The resistance of gears is equal to motor power of 3 KW. Reduction gear box was supplied from Yılmaz Redüktör Inc. (YDE- 22).

### 3.1.3.3. Heaters and coolers

In order to give the required heating power to the polymer, ceramic heater bands were used which give 3 watts per every cm<sup>2</sup> of the barrel surface. Heaters were divided in 3 sections. Every ceramic heater section is surrounded with a cover and air blowers were attached to every section for cooling action. Heaters and coolers were supplied by Safi Industrial Heating Elements Company.

### 3.1.3.4. Pressure Gauge

In order to see the pressure inside and at the wall of die, 0-350 bar pressure gauge was introduced which was supplied by Gefran Company.

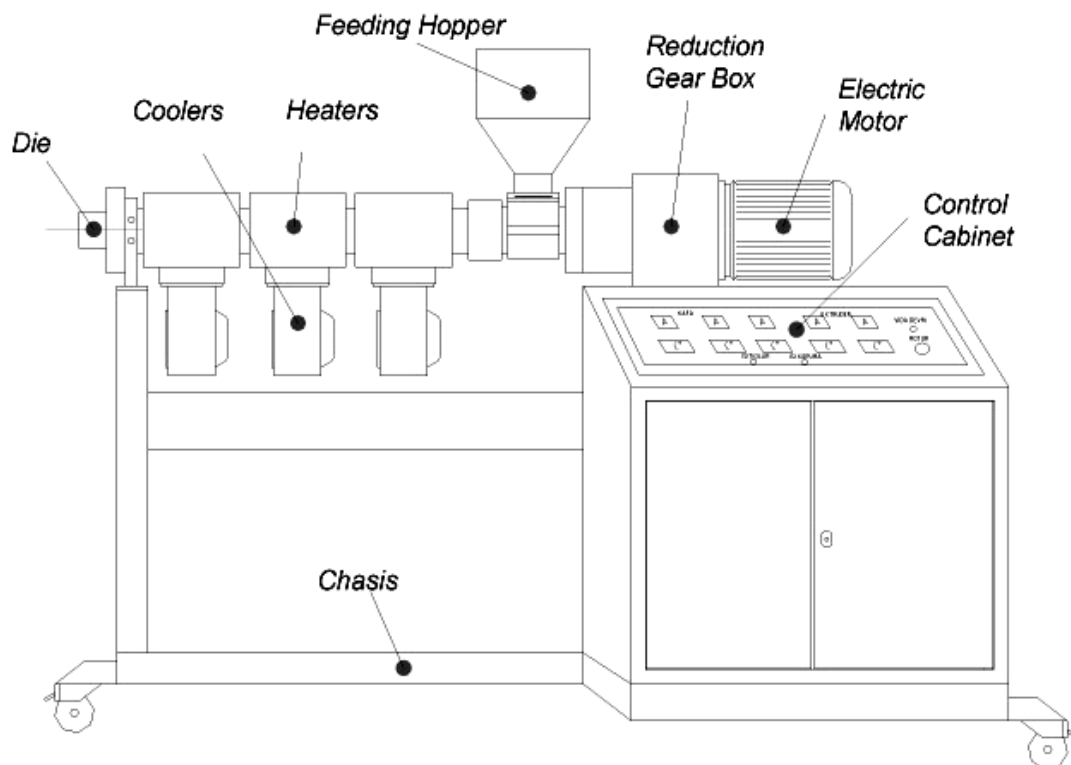


**Figure 3.3.** Components of the extruder

### **3.1.3.5. Control board**

All the controllers are introduced in a control board. Control board contains an AC motor inverter which can change the motor speed by adjusting the frequency. Temperature of the barrel measured by PT 100 sensors and controlled by PID (Proportional Integrated Distribution) controllers. Control board was supplied by Medel Electronic Company.

### **3.1.4. Construction of the Extruder**

The manufacturing of the screw and the barrel and the constructional work of the extruder were made in the workshop of Enformak Inc. The main components except the screw and the barrel were supplied by another firms but the construction of extruder was made in Enformak's workshop.

## **3.2. Experimental Study of Surface Irregularities**

The extruder, whose design definition was explained in section 3.1, was used for the investigation of the surface irregularities. Two different dies were used attached to the extruder. A die was used to have compounded strands and another rectangular slit die was used to carry out surface irregularities studies. The length of the land region of the slit die, L, is 28 mm, width of the die, W, is 25 mm and the thickness, H, is 1 mm.

### **3.2.1. Materials Used for Surface Irregularities Study**

#### **3.2.1.1 Low Density Polyethylene (LDPE)**

Low density polyethylene used is a commercial product of Petkim Petilen G 03-5 Petrochemical Co. Reported properties of G 03-5 by Petkim is  $M_n$  (g/mol) = 20.300,  $M_w$  (g/mol) = 213.600,  $HI$  (=  $M_w/M_n$ ) = 10.5,  $M_v$  (g/mol) = 133.300, light bimodal, highly branched.

#### **3.2.1.2 Commercial Polymer Processing Aid (PPA) Additives**

Fluorinated polymers based processing aids were supplied by Aksoy Plastics Corp. PE/F 108250 is a masterbatch consisting 5% Dyneon FX 5920 PPA and 95% carrier LDPE reported usage level 1%, reported benefits are to prevent melt fractures, die build-up, gel formations and surface defects. PE/F 108320 is a masterbatch consisting

2% Dyneon FX 9613 PPA and 98% carrier LDPE reported usage level 1-1.5% with similar benefits.

### **3.2.1.3 Silicone Based Additive**

The  $\alpha$ ,  $\omega$  dihydroxy polycaprolactone-poly (dimethylsiloxane) ( PCL-PDMS-PCL) triblock copolymer used was a commercial product Goldschmidt Chemical Corp. (Tegomer H-Si 6440 with  $M_n = 6500 \pm 600$ ;  $M_w$  (PDMS) = 3000; and PCL end blocks = 2000 g/mol).

## **3.2.2. Equipments**

### **3.2.2.1 Extruder**

The prepared extruder which is detailed above was used for the extrusion of samples. The general properties of the extruder are as follows; it is a single screw extruder to run for laboratory studies. The extruder has a universal single flight, 25 turns long, simple 3 stage screw. The screw speed can be adjusted up to 97 rpm. Three section for barrel and die temperatures can be adjusted by ceramic heaters and air blowers by means of PID controllers. The pressure before the die can be seen between 0-350 bar by the pressure gauge. In front of the extruder, a cooling bath and an adjustable speed take off unit was used.

### **3.2.2.2 Die**

Two different dies were used. One of them is slit die with the dimensions  $W=25\text{mm}$ ,  $L=28\text{mm}$ ,  $H=1\text{ mm}$  (see Fig.3.4) and a granulating die.

### **3.2.2.3 Melt Flow Index Equipment**

Execution of a MFR measurement was described in DIN ISO 1133 as procedure. The originally defined MFR method determines the sample mass flowing out in a defined time. The results were indicated g/10 min. MFR measurements were made under 2.16 kg load. Semi-Automatic Haake Melt Flow MT was used to carry out experiments.

### **3.2.2.4 Camera**

High resolution 5.1 mega pixel Sony DCR-W digital camera which has close-up mode was used to picture the surface conditions of the samples.

### 3.2.2.5 Parallel Plate Rheometer

TA instruments AR 2000 model rheometer has the geometry as 25 mm ETC aluminum parallel plate, 1000  $\mu\text{m}$  gap. Data and measurements were obtained by means of software program named “Rheology Advantage”.

### 3.2.3. Experimental Method

#### 3.2.3.1 Calculation of the Shear Stress

For the slit die that we have used, the shear stress value at the die wall was determined by ‘ $\tau = \Delta P W H / 2(W + H) L$ ’.  $\Delta P$  is the pressure before die in bars,  $W$  is width of the die in mm,  $H$  is the thickness of the die in mm,  $L$  is the land region length of the die in mm. Result will give us the die wall shear stress in MPa.

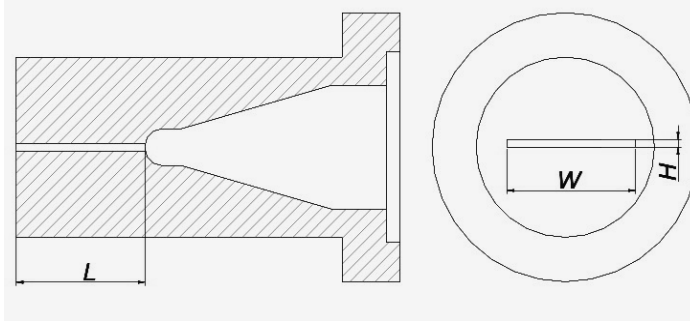


**Figure 3.4.** Shape of the slit die used.

#### 3.2.3.2 Determination of Critical Shear Stress Value

In order to determine the critical shear stress approximate value of 0.1, MPa that was stated in the literature was tested. For this purpose LDPE was extruded by the slit die under different extrusion rates. By applying different screw speed, different shear stress values were obtained. Surface properties of the obtained samples were observed. In two different temperatures profile tests were examined. Screw speed was increased step by step. At each step a sample was taken after the extrusion process stabilized. Each sample was observed to determine, at which degree of shear stress value the sharkskin melt fracture irregularities has started.

**Table 3.1** Temperature profile and extrusion data's of LDPE with 190 C° Die Temp.

<b>Die (C°)</b>	<b>3. Zone (C°)</b>	<b>2. Zone (C°)</b>	<b>1. Zone (C°)</b>
190	190	180	140
<b>Material</b>	<b>Screw Speed (r.p.m)</b>	<b>ΔP Die Pressure (Bar)</b>	<b>Calc. Shear Stress (MPa)</b>
LDPE	6	70	0,120
LDPE	10	90	0,154
LDPE	15	102	0,175
LDPE	20	110	0,188
LDPE	25	119	0,204
LDPE	30	125	0,214

**Table 3.2** Temperature profile and extrusion data of LDPE with 175 C° Die Temp.

<b>Die (C°)</b>	<b>3. Zone (C°)</b>	<b>2. Zone (C°)</b>	<b>1. Zone (C°)</b>
175	170	160	130
<b>Material</b>	<b>Screw Speed (r.p.m)</b>	<b>ΔP Die Pressure (Bar)</b>	<b>Calc. Shear Stress (MPa)</b>
LDPE	10	105	0,180
LDPE	15	120	0,206
LDPE	20	130	0,223
LDPE	25	138	0,236
LDPE	30	144	0,265
LDPE	44	161	0,276



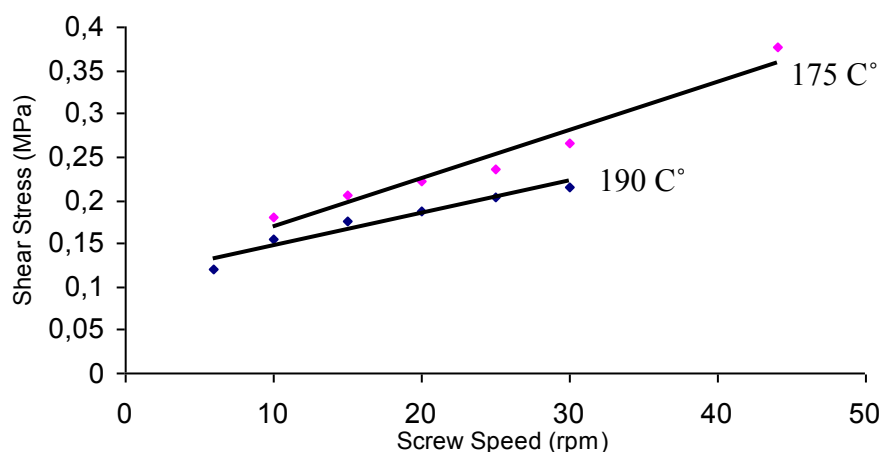


**Figure 3.5.** Shear stress vs. Screw speed graph for LDPE at 175 and 190 °C

### 3.2.3.3 Effects of Commercial Additives

In order to see the effect of commercial additives to the surface conditions of the extruded products under different shear stress value, fluorinated polymer based masterbatches were added in different ratios. Two different fluorinated polymer masterbatch PPA s PE/F 108320 and PE/F 108250 were tested under different shear stress values. Masterbatches were added to the polymer sample in desired ratios and they were mixed in a vessel properly. And the prepared mixtures were extruded in different shear rates.

**Table 3.3** Temperature profile and extrusion data of LDPE with different additive ratios.

	<b>Die (C°)</b>	<b>3. Zone (C°)</b>	<b>2. Zone (C°)</b>	<b>1. Zone (C°)</b>
<b>Temperatures</b>	185	180	175	140
<b>Material (LDPE With)</b>	<b>Screw Speed (r.p.m)</b>	<b>ΔP Die Pressure (Bar)</b>	<b>Calc. Shear Stress (MPa)</b>	<b>Output Rate (g/h)</b>
1500 ppm FX 5920	10	88	0,151	614
2500 ppm FX 5920	10	75	0,128	614
4000 ppm FX 5920	10	69	0,118	585
1500 ppm FX 5920	20	110	0,188	1392
2500 ppm FX 5920	20	90	0,154	1126
4000 ppm FX 5920	20	92	0,157	890

### 3.2.3.4 Effects of Silicone Based Additive

In order to see the effects of the Silicone Based H-Si 6440 to the surface conditions of extruded LDPE, we added H-Si 6440 to the LDPE in different ratios. First the H-Si 6440 beads were cut in smaller parts which have the similar sizes to LDPE beads to have a better mixing. Then both of the materials were mixed properly in a vessel. To have better distribution of the H-Si 6440 particles in LDPE matrix, we first extruded the LDPE – H-Si 6440 mixture in different ratios once with a granulating die. Then we extruded the mixtures with different shear rates

**Table 3.4** Temperature profile and extrusion data of LDPE- H-Si 6440 with different ratios and shear rates.

	<b>Die (C°)</b>	<b>3. Zone (C°)</b>	<b>2. Zone (C°)</b>	<b>1. Zone (C°)</b>
<b>Temperatures</b>	185	180	175	140
<b>Material (LDPE With)</b>	<b>Screw Speed (r.p.m)</b>	<b>ΔP Die Pressure (Bar)</b>	<b>Calc. Shear Stress (MPa)</b>	<b>Output Rate (g/h)</b>
500 ppm H-Si 6440	10	94	0,161	560
750 ppm H-Si 6440	10	96	0,164	610
500 ppm H-Si 6440	15	110	0,188	958
750 ppm H-Si 6440	15	110	0,188	952
500 ppm H-Si 6440	20	125	0,214	1314
750 ppm H-Si 6440	20	120	0,206	1276

### 3.2.3.5 Comparison of the Samples Regarding to Rheological Properties

The measurements of the rheological properties of samples were carried out by the plate-and-plate rheometer at 190 °C. All experiments were run at the range of 0.01-100 Hz frequency, 0.002-0.500 1/s shear rate, 200-15,000 (Pa) shear stress. Viscosity and modulus curves are derived from data, which is obtained working at the constant frequency and shear rate values.

## **4. RESULTS AND DISCUSSION**

### **4.1 Preparation of the laboratory extruder**

Prepared extruder was used for the surface irregularities studies. The anticipated requirements for the extruder were successfully obtained. The processed materials melted and gained the required pressure to get out of the die and to acquire the shape of the die. The whole control mechanism has run properly. It has been seen by different screw speed extrusion trials of LDPE that the calculated mass flow rate data were consistent with the experimental results (Table 4.1).

### **4.2 Determination of Critical Shear Stress Value**

In the literature, critical wall shear stress, at which surface irregularities appears is given as 0.1 MPa.[5] Up to 70 bar die pressure, almost no surface defect has been seen. After the 70 bar die pressure, the screw speed has been increased step by step. At all stages the extrusion process has been waited for a while to have a stable extrusion condition. Some small amplitude sharkskin melt fracture defect has been seen at the shear stress value of 0.154 MPa (Table 4.2). As we approach the 0.3 MPa, the surface irregularities increased markedly. (Figure 4.1) Because of some restrictions such as gross irregularities, temperature control problems we could not go further.

### **4.3 Effects of Commercial Additives**

In order to see the effects of the commercial processing aids to prevent surface irregularities, we used Dyneon processing aids in different ratios. We have performed experiments above the critical shear stress point. For this purpose, PE/F 108250 were used as a PPA (Polymer Processing Aid). In this masterbatch 5 % FX 5920 are included. If 1 % PE/F 108250 were added to the system 500 ppm FX 5920 should be added. Advised usage level for the PE/F 108250 is 1%, but we have seen that; 1% did not help to remove melt fracture in short time. Then 3 % of PE/F

108250 (1500 ppm FX5920), 5% of PE/F 108250 (2500 ppm FX5920) and 8 % of PE/F 108250 (4000 ppm FX5920) additive levels has been tried. It is advised from the masterbatch producer that; PPA can affect the process barely 20 minutes later from the start. It has been seen that; PPA's effect has appeared increasingly in 25 minutes. By the melt fracture decreasing with time, melt pressure also decreased. It has also been seen that; the output rate of the extruder also decreased by time and by decreasing pressure (Table 4.3). On the other hand PE/F 108320 showed the similar effects.

#### **4.4 Effects of Silicone based additive**

The used Commercial Processing aids contain fluoro polymers. The surface tension - which is one of the important parameters for the surface irregularities- of the fluoro containing polymers is closer to that of siloxane containing polymers than the others. For this reason we tried the siloxane containing commercial additive as a PPA.

Silicone based additive H-Si 6440 has been added to the LDPE in different ratios. Every mixture has been tested with various screw speed. 500 ppm, 750 ppm, 1000 ppm silicone containing additive has been tested under different shear stresses (Table 4.4). It has been seen that, adding the H-Si 6440 to the LDPE has improved the surface conditions of the LDPE extrudates after the critical shear stress point (Figure 4.2). But it has seen that the mixture which is containing more than 750 ppm is not affecting the extrudate positively. Extrudate has become unstable and the additive content becomes a separate phase and accumulating on the surface when the content of H-Si 6440 in the mixture higher than 750 ppm.

#### **4.5 MFR Measurements**

MFR measurement is one of the test methods used to understand the flow properties of the material. Since the polymers flow easily when they have higher MFR values, the surface irregularities will be less. The surface irregularities will be expected to appear at lower shear stress values, when the MFR value of the material is lower. More over, increment in the percentage of the Dyneon additive in LDPE, resulted with the increment in the measured MFR and MVR values. When we compare samples with pure LDPE, it can be seen that; MFR, MVR values of both of the

samples with Dyneon additive has higher values than pure LDPE. It has been seen that the MFR or MVR values of the LDPE mixtures with Dyneon PPA and H-Si 6440 additives have slightly been increased. The change in melt index of the mixtures has been expected to be higher than it was. The cause of this slight difference could be the short duration of the melt index measurement. The extrusion studies showed that, the complete influence of effects of the commercial additive and the H-Si 6440 additive take at least 30 -35 minutes. Moreover; it has been seen that, the increment in the Dyneon PPA quantity resulted as increment of MFR and MVR values. When these results have been compared with pure LDPE, it has been seen that MFR and MVR values of both samples are higher than that of virgin LDPE. MFR and MVR tests of H-Si 6440 are resulted as similar with the others and the increment in H-Si 6440 quantity is resulted as an increment in MFR and MVR values. It has been seen that both of these values are higher than the pure LDPE values, but the quantity of H-Si 6440 is lower than the Dyneon PPA for similar results. In connection, when it has been compared in terms of shear stresses, it has been observed that, in the same screw speed levels die pressure values of H-Si 6440 and so the shear stress values are higher.

#### **4.6 Rheological Properties**

The flow behavior of the most thermoplastics does not follow Newtonian Law of viscosity. Polymeric melts are pseudoplastic fluids. In order to determine the Newtonian and power law regions of the polymeric fluids, viscosity versus Shear stress or shear rate curves are obtained from the rheological measurements which are obtained at 190°C. Newtonian region is seen at very low shear rate values and the viscosity in this region is constant. Zero shear viscosity can be measured from Newtonian region. In the Power Law region, viscosities decrease with increasing of shear rate.

From the data obtained, viscosity vs. shear rate, viscosity vs. shear stress, shear stress vs. shear rate, storage modulus ( $G'$ ) vs. angular frequency, loss modulus ( $G''$ ) vs. angular frequency,  $G'$  vs.  $G''$ , and complex viscosity ( $|\eta^*|$ ) vs. angular frequency.

In the viscosity-shear rate curve of LDPE (Figure 4.3), at the low shear rate values pure LDPE has the lowest viscosity value. The addition of additives increased the viscosity of polymer. Especially addition of H-Si 6440 markedly increased the

viscosity of polymer at low shear rate values. The zero shear viscosities can be seen from this low shear rate (Newtonian region), and the calculated zero shear viscosities of LDPE, FX 5920 and H-Si 6440 are respectively 58380, 68300, 85840 Pa.s. At higher shear rate values, difference between H-Si 6440 and the others is lower and FX 5920 has the lowest viscosity. Power Law index ( $n$ ) values were calculated from Power Law region by the help of Eqn. 2.5 and zero shear viscosity values were determined from Newtonian region. There is no significant difference between the power law indexes of all three samples. The power law indices of LDPE and H-Si 6440 containing LDPE is 0.40 and the FX 5920 containing LDPE power law index is 0.39. It can be said that samples exhibit shear thinning (pseudo plastic) behavior, since the Power Law indices ( $n$ ) are less than 1.

Viscosity - shear rate curve showed the similar behavior with the viscosity-shear stress curve with more clear differences. (Figure 4.4)

In the Shear stress – Shear rate plot, it has been seen that; the differences between the shear stress values are getting lower by the increasing shear rate (Figure 4.5). The 750 ppm H-Si 6440 containing LDPE has the highest shear stress values both low and high shear rates as it is in figures 4.3 and 4.4.

At the low frequencies, storage modulus ( $G'$ ) values of LDPE and 750 ppm H-Si 6440 higher than those of 1500 ppm FX 5920. It means that their elasticities are higher than that of 1500 ppm FX 5920. It shows that the addition of FX 5920 makes lower the elasticity of LDPE while the additions of H-Si 6440 do not affect so much. At the high frequencies, between 0.5 and 40 rad/s., elasticity of all samples are almost the same. Above the 40 rad/s. it's expected that the behavior of the samples are opposite of the lower frequencies (Figure 4.6).

Loss modulus ( $G''$ ) value of 1500 ppm FX 5920 is lower than those of pure LDPE and 750 ppm H-Si 6440 at frequencies until 0.5 rad/s. At higher frequency rates loss modulus values of 750 ppm H-Si 6440 shows the lowest value. It can be seen from the figure 4.6 and figure 4.7 that, the storage modulus ( $G'$ ) and the loss modulus ( $G''$ ) of all samples are almost same at the frequency of 0.5 rad/s (Figure 4.7).

There are some small changes up to the point of 0.5 rad/s frequency value on the plot of  $G'$  vs  $G''$ . The graphic is very nearly linear after the frequency value of 0.5 rad/s.

It means that there is no change in the value of  $G'$  vs.  $G''$  for all three samples (Figure 4.8).

At low frequencies under the 0.5 rad / sec the complex viscosity value of the 1500 ppm FX 5920 containing LDPE is lower than the others. But after 0.5 rad/sec, all the samples have almost the same complex viscosity values versus to frequencies (Figure 4.9).

#### **4.7 Conclusion**

The anticipated requirements for the manufactured extruder such as capacity and the functionality were successfully obtained and it used for surface irregularities properly. The critical shear stress value of 0.1 MPa which is reported in literature has been seen for LDPE. Several different PPA has been examined, and FX 5920 compared with the novel PPA H-Si 6440 regarding to surface irregularities. With the same processing conditions and the same screw speeds. H-Si 6440 gave the higher output and higher pressures but the similar clearance effects for surface irregularities with the lower additive usage level. (Figure 4.2, table 4.2, 4.3). It has also been seen that both samples have higher MFR values than the pure LDPE has, and there is no significant difference among results. The rheometer results showed that; all the samples showed the pseudoplastic behavior and both of the samples has higher zero shear viscosity, and the H-Si 6440 has the highest one. The 0.5 rad/s frequency value showed a boundary on the all plots. It shows the transition point of the samples to the pseudoplastic behavior, and it's almost same for both additives and they are higher than pure LDPE. The power-law index calculated from the pseudoplastic region of the shear stress – viscosity plot and all three values are almost same. As a result we can say that H-Si 6440 can be used as an alternative PPA for the clearance of surface irregularities.



## REFERENCES

- [1] **Simonds, H.R.**, 1964, A Concise Guide to Plastics, Reinhold Publishing Corporation, New York.
- [2] **Rauwendaal, C.**, 2001, Polymer Extrusion Carl Hanser Verlag, Munich
- [3] **Baird, D.G., Collias, D.I.**, 1998, Polymer Processing Principles and Design, John Wiley & Sons, Inc., New York
- [4] **Modern Plastics Encyclopedia**, 1985-1986, McGraw-Hill Inc. New York
- [5] **C. J. S. Petrie and M. M. Denn**, 1976, A I ChE J., 209-236.
- [6] **Tordella J.P.**, 1958, An Instability in the Flow of Molten Polymers, *Rheol. Acta*, **1**, 216–221.
- [7] **Den Otter J.L.**, 1970, Mechanisms of melt fracture. *Plastics & Polymers*, June:155–168
- [8] **Weill A .**, 1980, About the origin of sharkskin. *Rheol. Acta* **19**, 623–632
- [9] **Howells E.R., Benbow J.J.**, 1962, Flow defects in polymer melts. *Trans J Plastics Inst* **30**, 240–253
- [10] **Kurtz S.J.**, 1984, Die geometry solutions sharkskin melt fracture. *Proc IX Intl Congress on Rheol.*, Mexico, pp 399–407
- [11] **Ramamurthy, A.V.**, 1986, “Wall slip in viscous fluids and influence of materials of construction,” *J. Rheol.* **30**, 337–357
- [12] **Kalika D.S., Denn M.M.**, 1987, Wall slip and extrudate distortion in linear low-density polyethylene. *J. Rheol.* **31**, 815–834
- [13] **Person T.J., Denn M.M.**, 1997, The effect of die materials and pressure-dependent slip on the extrusion of linear low-density polyethylene. *J. Rheol.* **41**, 249–265
- [14] **Piau, J. M., N. El Kissi, F. Toussaint, and A. Mezghani**, 1995a, Distortions of polymer melts and extrudates and their elimination using slippery surfaces, *Rheol. Acta* **34**, 40–57

- [15] **Piau, J. M., N. Kissi, and A. Mezghani**, 1995b, "Slip flow of polybutadiene through fluorinated dies," *J. Non-Newtonian Fluid Mech.*, **59**, 11–30
- [16] **Hatzikiriakos S.G., Dealy J.M.**, 1991, Wall slip of molten high density polyethylene. I. Sliding plate rheometer studies., *J. Rheol.*, **35**, 497–523
- [17] **Hatzikiriakos S.G., Dealy J.M.**, 1992, Wall slip of molten high density polyethylene. II. Capillary rheometer studies. *J. Rheol.* **36**, 703–741
- [18] **Beaufils P., Vergnes B., Agassant J.F.**, 1989, Characterization of the sharkskin defect and its development with the flow conditions. *Intern Polym Processing*, **IV**, 78–84
- [19] **Piau J.M., El Kissi N., Tremblay B.**, 1990, Influence of upstream instabilities and wall slip on melt fracture and sharkskin phenomena during silicones extrusion through orifice dies. *J. Non-Newtonian Fluid Mech* **34**, 145–180
- [20] **Piau J.M., El Kissi N., Toussaint F., Mezghani A.**, 1995, Distortions of polymer melt extrudates and their elimination using slippery surfaces. *Rheol. Acta* **34**, 40–57
- [21] **Hatzikiriakos S.G., Dealy J.M.**, 1993, Effects of interfacial conditions on wall slip and sharkskin melt fracture of HDPE. *Intern Polymer Processing* **VIII**, 36–43
- [22] **El Kissi N., Leger L., Piau J.M., Mezghani A.**, 1994, Effect of surface properties on polymer melt slip and extrusion defects. *J.Non-Newtonian Fluid Mech.***52**, 249–261
- [23] **Hatzikiriakos S.G., Hong P., Ho W., Stewart C.W.**, 1995, The effect of Teflon coatings in polyethylene capillary extrusion. *J. Appl Polym Sci* **55**, 595–603
- [24] **La-Mantia, F.P., C. Geraci, M. Vinci, U. Pedretti, A. Roggero, L.I. Minkova, and P.L. Magagnini**, 1995, "Morphology and properties of blends of polyethylene with a semiflexible liquid crystalline polymer," *J. Appl. Polym. Sci.* **58**, 911–921.
- [25] **Herdle, W.B. and W.A. Fraser**, 1987, "Improvements in blown film extrusion of polyolefins containing a novel processing aid," ANTEC 87, New York, N.Y., pp. 1268–1270
- [26] **Schumacher, P.A.**, 1986, "Novel processing aid for greater flexibility in blown film extrusion," *SPI/SPE 86 Plastics South Conference Proceedings*, Atlanta, GA, pp. 78–82.

- [27] **Rudin, A., A.T. Worm, and J.E. Blacklock**, 1985a, “Fluorocarbon elastomer processing aid for LLDPE, HDPE and PP resins,” Processing and Property Enhancement Utilizing Modifiers and Additives in Polymer, *First International Conference*, Newark, New Jersey, Society of Plastics Engineers, Brookfield Center, CT, pp. 71–81.
- [28] **Rudin, A., A.T. Worm, and J E. Blacklock**, 1985b, “Fluorocarbon elastomer processing aid in film extrusion on linear low density polyethylenes,” *J. Plast. Film Sheeting* **1**, 189–204.
- [29] **Rudin, A., S. Nam, A.T. Worm, and J.E. Blacklock**, 1986, “Improvements in polyolefin processing with a fluorocarbon elastomer processing aid,” ANTEC 86, Boston, MA, pp. 1154–1157
- [30] **De Smedt, C.D. and S. Nam**, 1987, “The processing benefits of fluoroelastomer application in LLDPE,” *Plastics and Rubber Processing and Applications* **8**, 11–16.
- [31] **Klein, D.F.**, 1987, “The effects of a fluorocarbon elastomer processing aid on the blown film extrusion of linear low density polyethylene - Polyolefins V Session C: Polyolefin additives!,” RETEC Polyolefins V: *Fifth International Conference on Polyolefins*, Houston, TX, Society of Plastics Engineers, Brookfield Center, CT, pp. 285–300.
- [32] **Johnson, B. and J. Kunde**, 1988, “The influence of polyolefin additives on the performance of fluorocarbon elastomer process aids,” ANTEC 88, Atlanta, Ga, pp. 1425–1429.
- [33] **Cogswell, F.N.**, 1977, “Stretching flow instabilities at the exits of extrusion dies,” *J. Non-Newtonian Fluid Mech.* **2**, 37–47.
- [34] **Wang, S.Q., P.A. Drda, and Y W. Inn**, 1996, “Exploring molecular origins of sharkskin, partial slip, and slope change in flow curves of linear low density polyethylene,” *J. Rheol.* **40**, 875–898.
- [35] **Inn, Y.W., R.J. Fischer, and M.T. Shaw**, 1998, “Visual observation of development of sharkskin melt fracture in polybutadiene extrusion,” *Rheol. Acta* **37**, 573–582.
- [36] **Migler, K.B.; Son, Y.; Qiao, F.; Flynn, K.** 2002 *J. Rheol.* **46**, 383–400.

## APPENDIX . TABLES OF EXPERIMENTAL RESULTS

**Table 4.1.** Calculated and experimental mass flow rate data.

<b>Screw Speed (r.p.m)</b>	<b>Calculated Specific Capacity (g/h)</b>	<b>Calculated Capacity for screw speed (g/h)</b>	<b>Experimental Capacity (g/h)</b>
8	63	504	516
10		631	710
20		1260	1310

**Table 4.2.** Surface conditions of LDPE at different shear stress

Die (C°)	3. Zone (C°)	2. Zone (C°)	1. Zone (C°)	
190	190	180	140	
Material	Screw Speed (r.p.m)	$\Delta P$ Die Pressure (Bar)	Calc. Shear Stress (MPa)	Surface Condition Comment
LDPE	6	70	0,120	Almost no surface defect
LDPE	10	90	0,154	Some small sharkskin effect started
LDPE	15	102	0,175	Sharkskin effect has been seen
LDPE	20	110	0,188	Sharkskin effect has been seen
LDPE	25	119	0,204	Sharkskin effect markedly increased
LDPE	30	125	0,214	Sharkskin effect markedly increased
LDPE	44	161	0,276	Extrudate unstable, Gross irregularities near

**Table 4.3.** Surface conditions of LDPE – Dyneon additives mixture at different shear stress

	<b>Die (C°)</b>	<b>3. Zone (C°)</b>	<b>2. Zone (C°)</b>	<b>1. Zone (C°)</b>
<b>Temperatures</b>	185	180	175	140
<b>Material (LDPE With)</b>	<b>Screw Speed (r.p.m)</b>	<b>ΔP Die Pressure (Bar)</b>	<b>Calc. Shear Stress (MPa)</b>	<b>Output Rate (g/h)</b>
1500 ppm FX 5920	10	88	0,151	614
2500 ppm FX 5920	10	75	0,128	614
4000 ppm FX 5920	10	69	0,118	585
1500 ppm FX 5920	20	110	0,188	1392
2500 ppm FX 5920	20	90	0,154	1126
4000 ppm FX 5920	20	92	0,157	890

**Table 4.4.** Surface conditions of LDPE – H-Si 6440 additives mixture at different shear stress

	<b>Die (C°)</b>	<b>3. Zone (C°)</b>	<b>2. Zone (C°)</b>	<b>1. Zone (C°)</b>
<b>Temperatures</b>	185	180	175	140
<b>Material (LDPE With)</b>	<b>Screw Speed (r.p.m)</b>	<b>ΔP Die Pressure (Bar)</b>	<b>Calc. Shear Stress (MPa)</b>	<b>Output Rate (g/h)</b>
500 ppm H-Si 6440	10	94	0,173	560
750 ppm H-Si 6440	10	96	0,177	610
500 ppm H-Si 6440	15	110	0,203	958
750 ppm H-Si 6440	15	110	0,203	952
500 ppm H-Si 6440	20	125	0,231	1314
750 ppm H-Si 6440	20	120	0,221	1276

**Table 4.5.** MFR and MVR results of the LDPE, FX 5920 and H-Si 6440 mixtures.

<b>MATERIAL</b>	<b>MFI (g/10 min)</b>	<b>MVR (cm<sup>3</sup>/10 min)</b>
LDPE	0,26	0,34
1500 PPM FX 5920	0,29	0,38
2500 PPM FX 5920	0,30	0,39
500 PPM H-Si 6440	0,28	0,37
750 PPM H-Si 6440	0,29	0,38



## APPENDIX . FIGURES OF EXPERIMENTAL RESULTS

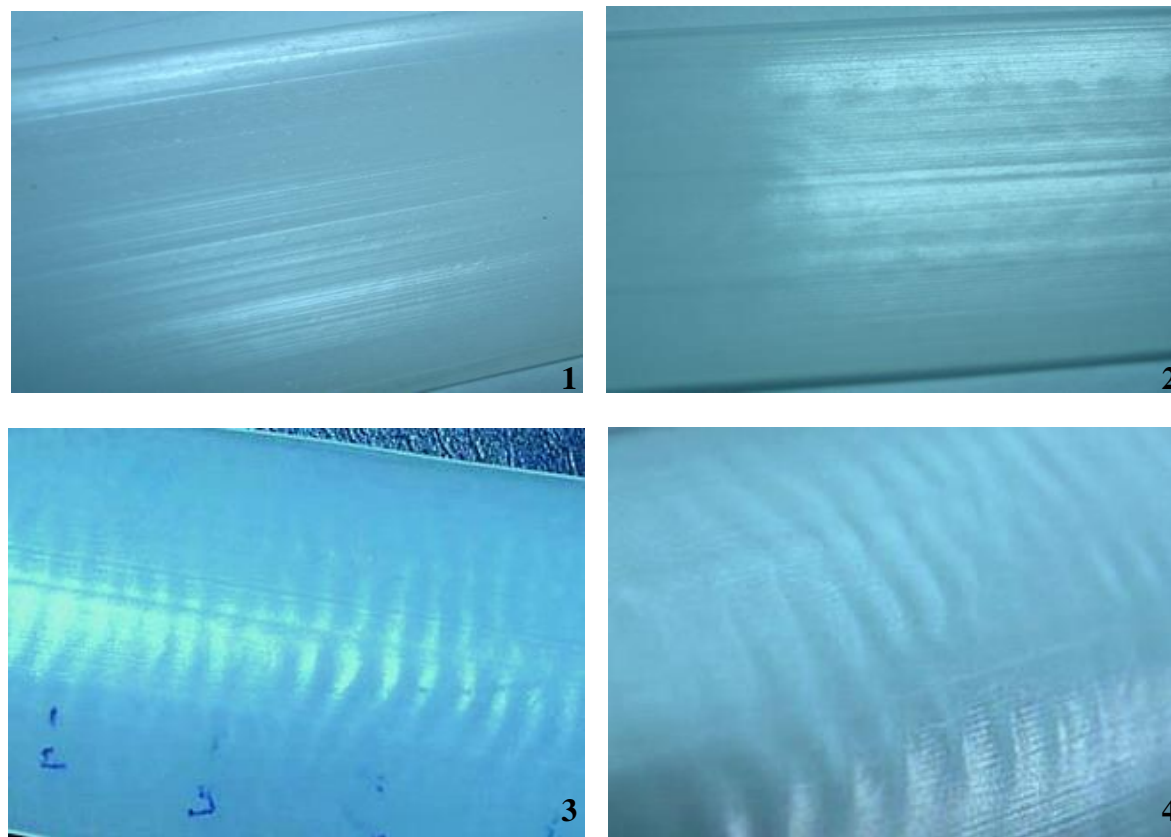


**Figure 4.1.** Surface appearance of the extruded LDPE slits in different die pressures. 1; 70 Bar, 2; 90 Bar, 3; 110 Bar, 4; 161 Bar

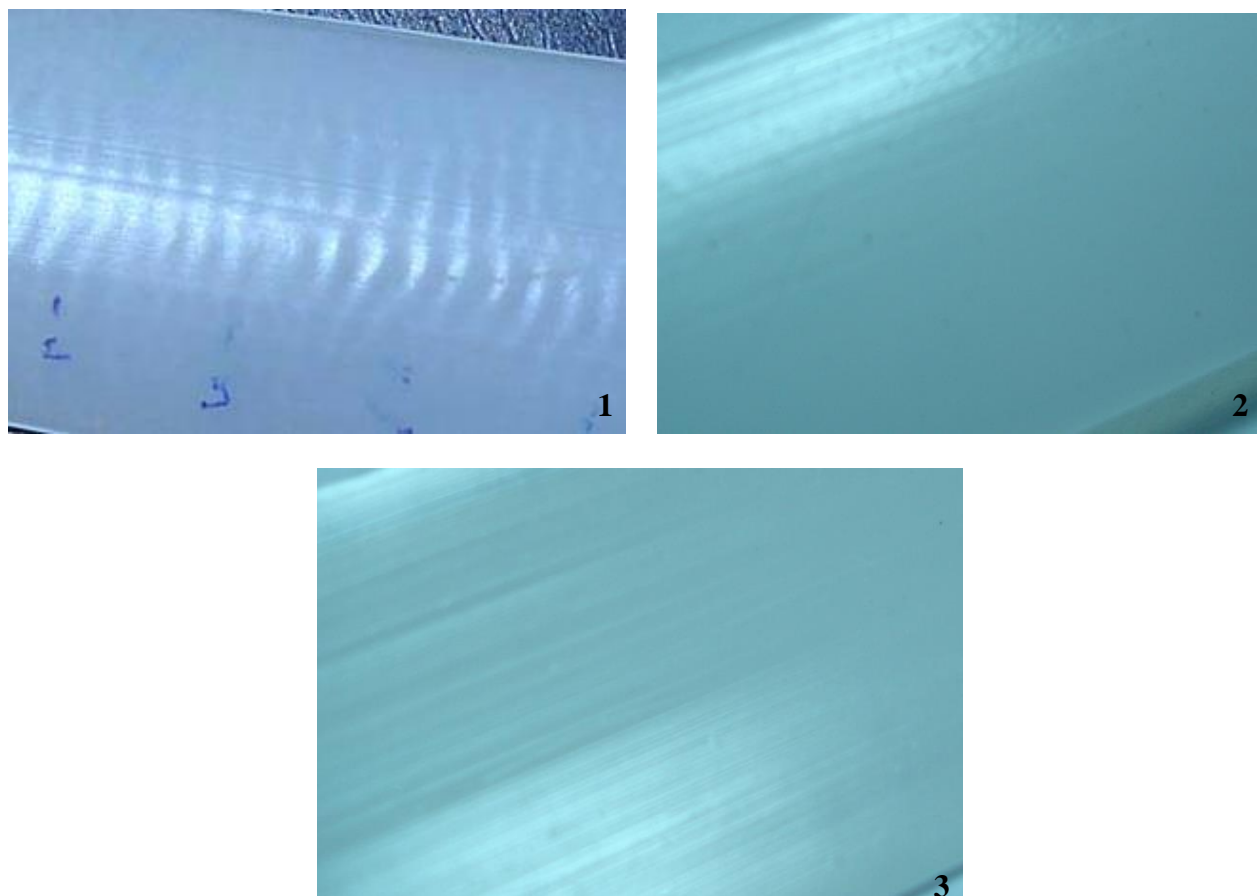


**Figure 4.2.** Surface appearance of the extruded samples in same shear stress point 1. LDPE at 110 Bar, 2.1500 PPM FX 5920 at 110 Bar, 3.750 PPM H-Si 6440 at 110 bar.

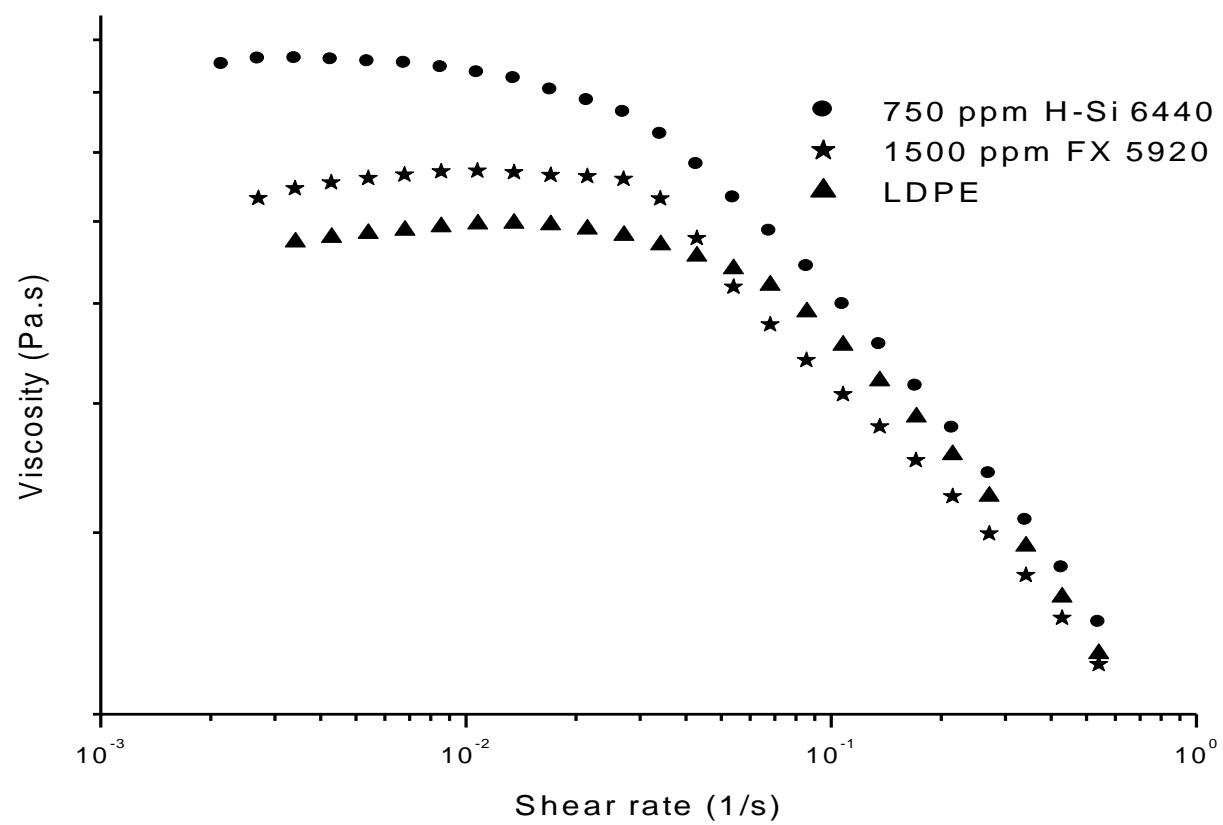


**Figure 4.3.** Viscosity vs. shear rate plot

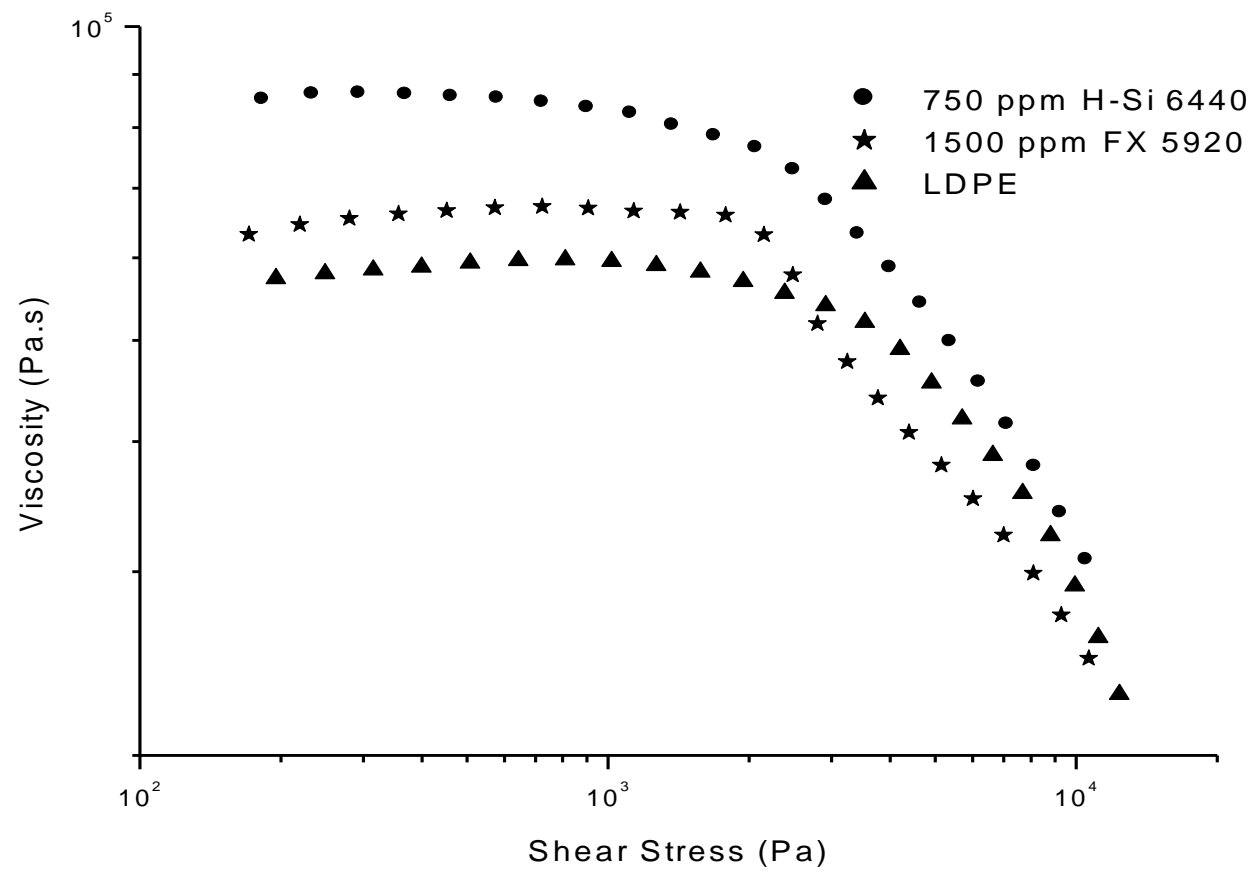


**Figure 4.4.** Viscosity vs. shear stress plot

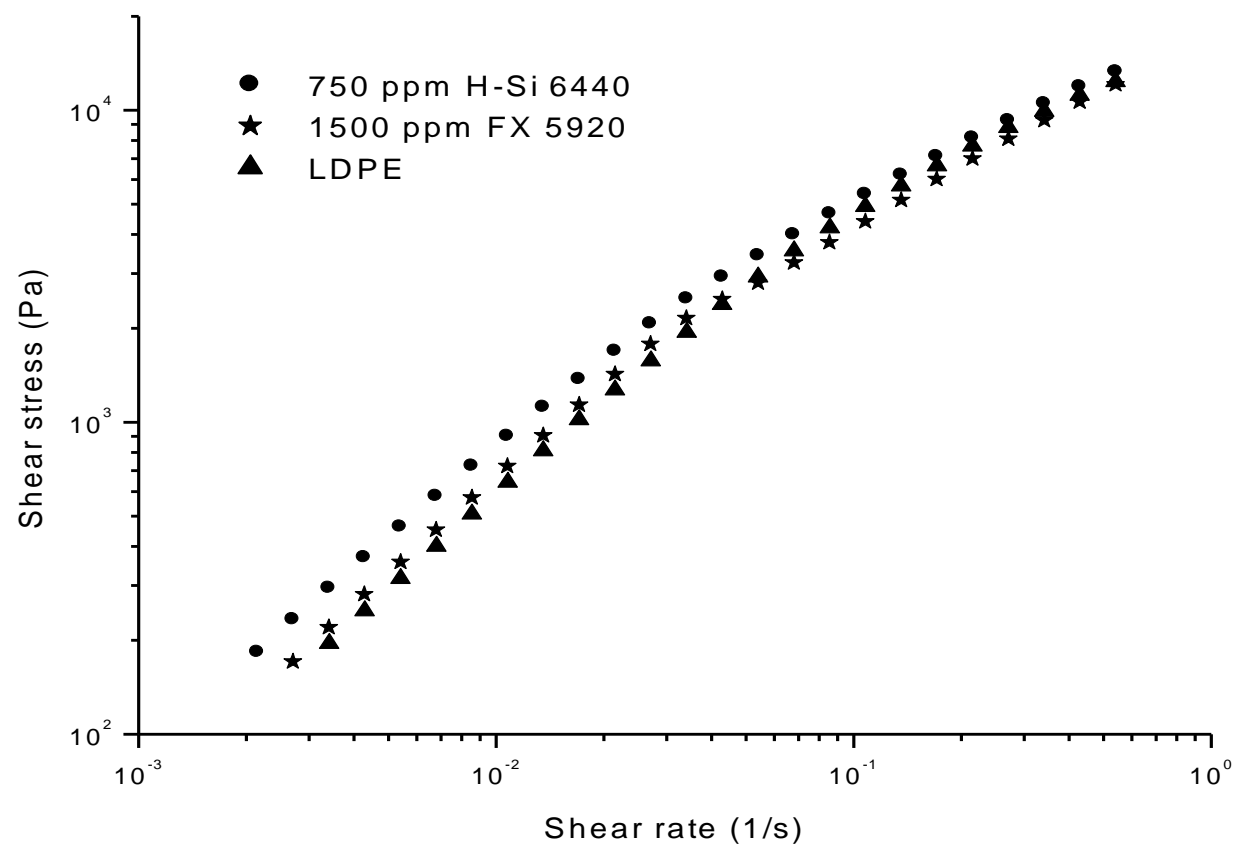


**Figure 4.5.** Shear stress vs. Shear rate plot

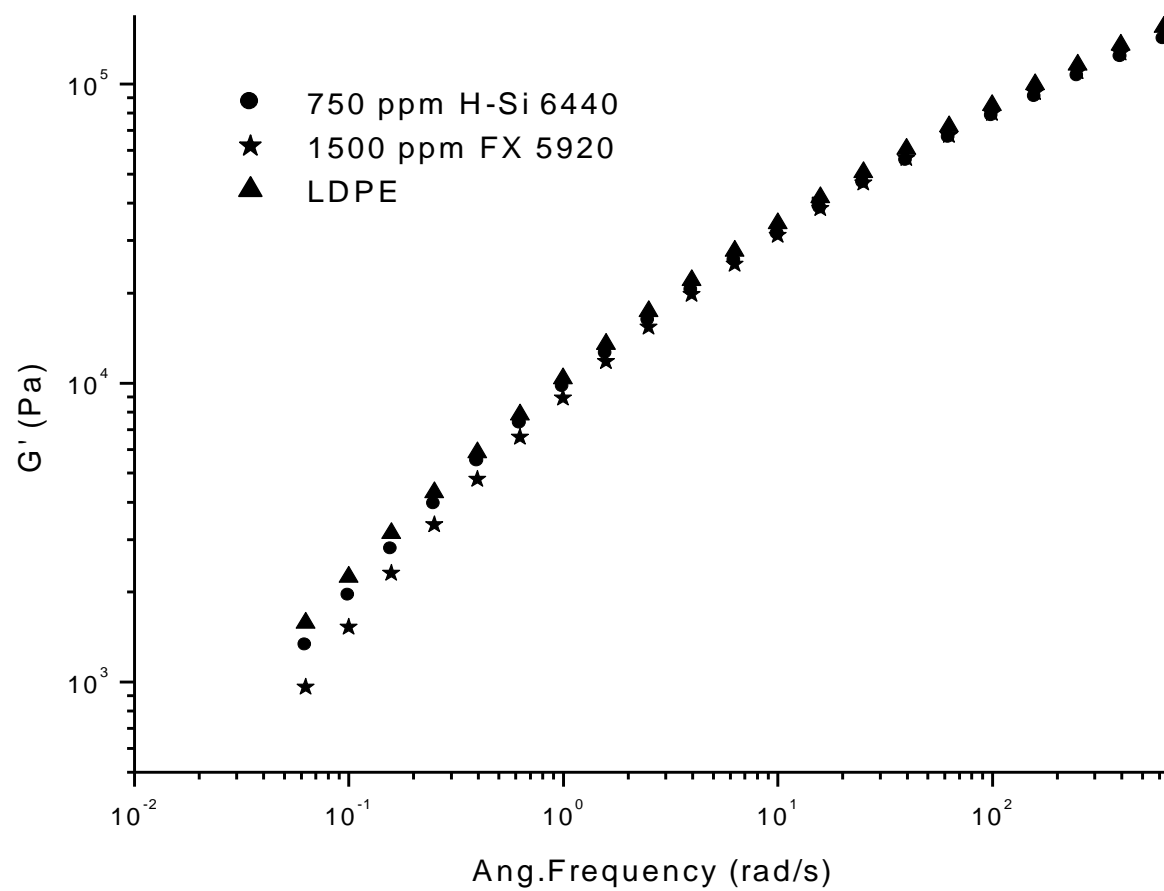


**Figure 4.6.** Storage modulus  $G'$  vs. Angular frequency e plot

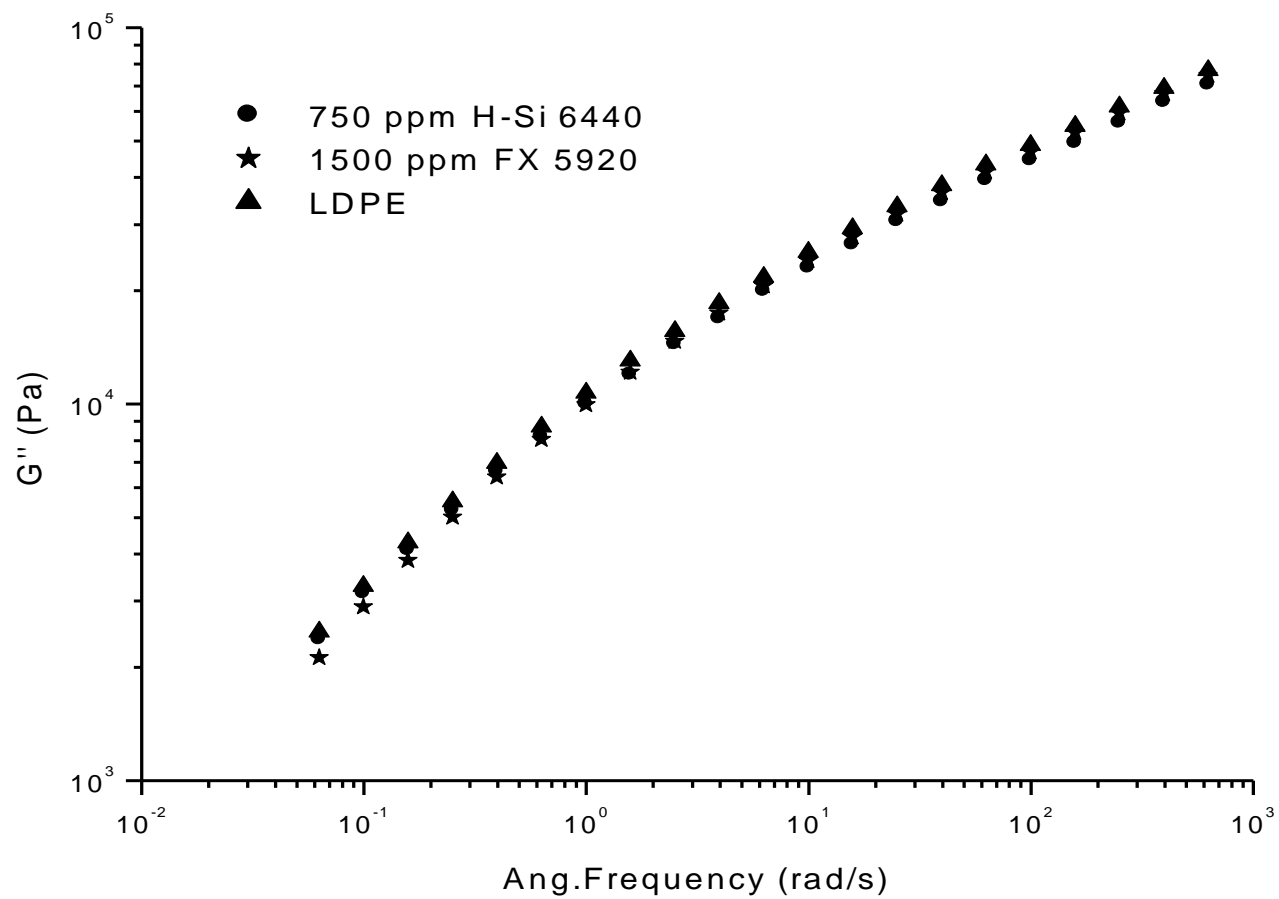


**Figure 4.7.** Loss modulus  $G''$  vs. Angular frequency e plot

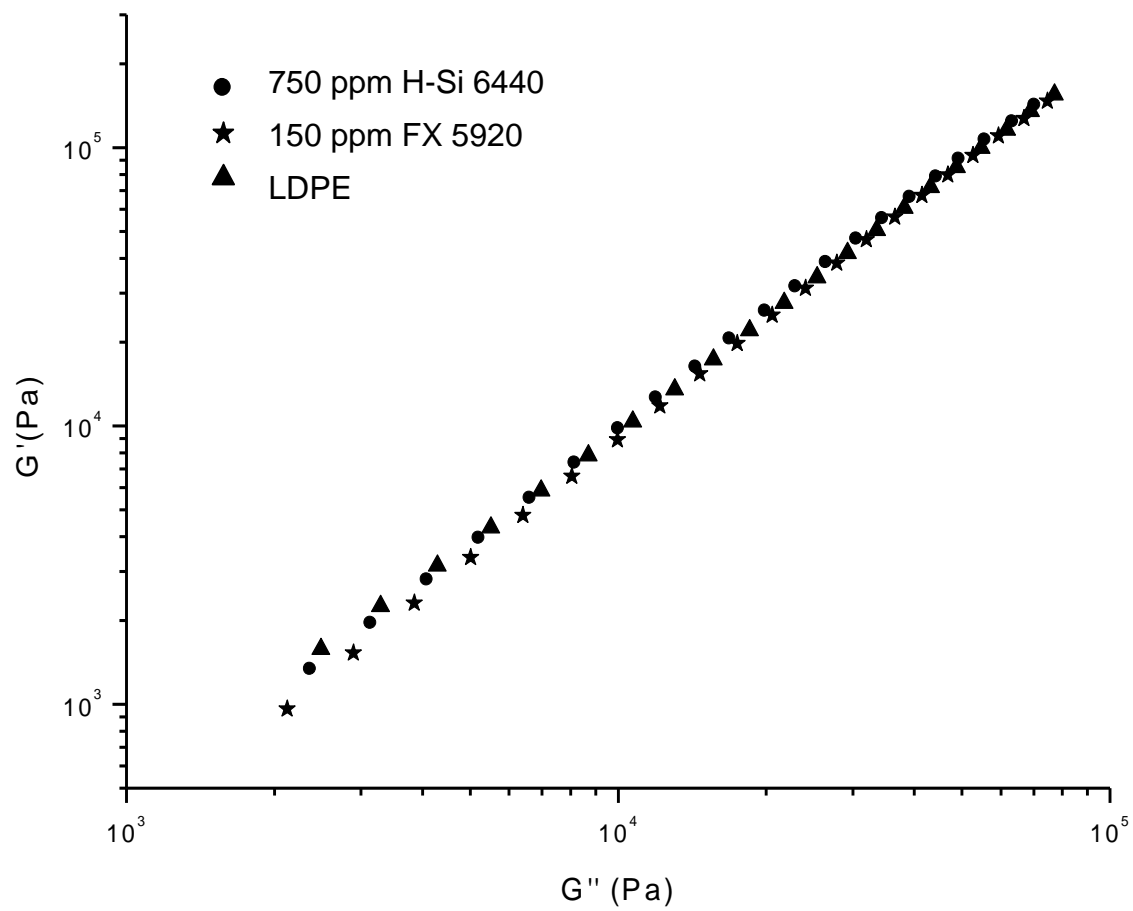


**Figure 4.8.** Storage modulus  $G'$  vs. loss modulus  $G''$  plot



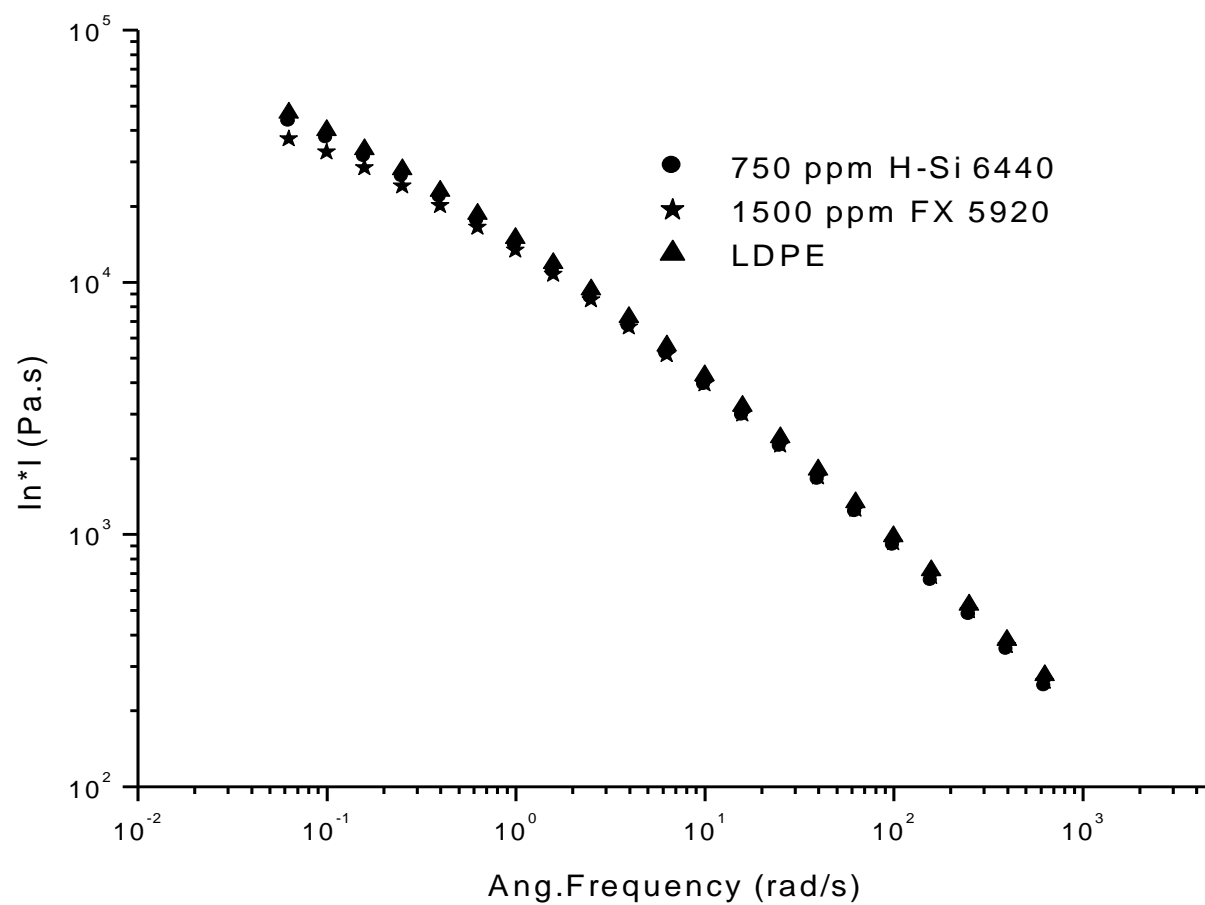


**Figure 4.9.** Complex viscosity  $|\eta^*|$  vs. Angular frequency plot

## **CURRICULUM VITAE**

He was born in Istanbul in 1978. He finished primary school, secondary school, and high school in Istanbul. In 1995, he attended the Physics Department of the Faculty of Science, University of Ankara. He finished his education here in 1999. After his training period in various firms, in 2000 he started to work for Enformak Inc. where he still has an active position in technical department. In 2001, He was accepted to the “Polymer Science and Technology” Master’s Degree Program of The Institute of Science in Istanbul Technical University.